UNIVERSITY OF MANITOBA

TRANSIENTS IN PLATES AND SHELLS OF REVOLUTION

by

DAVID PATHMASEELAN THAMBIRATNAM

A Thesis

PRESENTED TO THE FACULTY OF GRADUATE STUDIES
IN PARTIAL FULFILLMENT OF THE REQUIREMENTS FOR THE DEGREE OF

DOCTOR OF PHILOSOPHY

CIVIL ENGINEERING DEPARTMENT

WINNIPEG, MANITOBA
CANADA

JUNE 1978

TRANSIENTS IN PLATES AND SHELLS OF REVOLUTION

BY

DAVID PATHMASEELAN THAMBIRATNAM

A dissertation submitted to the Faculty of Graduate Studies of the University of Manitoba in partial fulfillment of the requirements of the degree of

DOCTOR OF PHILOSOPHY

TO MY PARENTS

MR. AND MRS. P.J. THAMBIRATNAM

ABSTRACT

The propagation of transient waves in linear, elastic, isotropic and homogeneous plates and shells of revolution is treated in this thesis. The analysis is based on the concept of a wave as a carrier of discontinuities in the field variable and/or its derivatives. The one to one relationship that exists between a particular transient problem and the corresponding time harmonic problem is first established and then exploited. This relationship makes it possible to deal with transient problems in terms of asymptotic series expansions, thereby making the analysis very much simpler than the usual method of discontinuity analysis.

The transient problems considered are due to impulsive loads acting at the boundaries of structures and specified in the form of strain, velocity or acceleration boundary conditions. Several numerical examples are solved to illustrate the method of solution as well as to establish its validity. The results are compared with existing solutions, wherever possible, and we obtain excellent agreement. A numerical superposition technique is developed which makes it possible to treat transient problems due to boundary loads of longer duration. This technique is applied to solve the problems of transient wave propagation in cylindrical shell structures subjected to ground excitation.

ACKNOWLEDGEMENTS

During my period of research at the University of Manitoba, I have been very fortunate in having Dr. A.H. Shah as my thesis advisor. I wish to acknowledge his expertise in all areas pertaining to my work and his personal interest in my progress. Dr. Shah was always willing to help and at times went out of his way to do so. For all this, and for the excellent guidance and encouragement that I received, I wish to express my sincere gratitude by saying "Thank you Dr. Shah, I couldn't have made it without you".

The early part of my research was done under the expert guidance of Dr. H. Cohen, who is my co-advisor. Dr. Cohen was always encouraging and gave me valuable suggestions and ideas. I wish to thank him for all the help that I received. I consulted Dr. P.N. Shivakumar whenever I was confronted with a problem that needed the expertise of a mathematician. I would like to thank Dr. Shivakumar for the help that he gave most willingly.

Mrs. Valerie Ring, who typed this thesis, has done an excellent job. She was very co-operative and understanding in doing the typing in such a short time. My sincere thanks are due to her.

I have been able to complete my Ph.D. program primarily due to the untiring efforts of my father-in-law Dr. Albert Vethanayayam, who has been a tremendous help to me at all times. He underwent great trouble, expense and even humiliation in order to overcome the numerous difficulties that I had pertaining to my stay in Canada. I wish to express my sincere gratitude for all this, and especially for the encouragement and moral support that I received in times of need.

I will fail in my duty if I did not thank my wife Sulogini and my little son Preshan. For my sake they willingly put up with several hardships away from our home country. I have to appreciate this even more, as Sulogini was almost a new bride when I started my program in Canada, and baby Preshan was born during the height of my work. They were very patient and understanding at all times, especially when there seemed to be "no end" to my program. Sulogini and Preshan accepted every situation cheerfully and always made the best out of it. I am deeply indebted to say "Thank you Sulo and thank you Presho, I appreciate your loyality, we'll have better times ahead".

I pursued my Ph.D. program as a Canadian Commonwealth Scholar and I wish to gratefully acknowledge the financial support of the Canadian Commonwealth Scholarship Committee.

TABLE OF CONTENTS

LIST OF FIGURES

CHAPTER I

INTRODUCTION

The problems of the propagation of transient waves in linear, elastic, isotropic and homogeneous plates and shells are treated in this dissertation. In the case of shells, consideration is restricted to shells of revolution with straight line generators. The transient waves that we consider are due to time dependent loads acting at the boundaries of the structure and specified in the form of strain, velocity or acceleration boundary conditions. Though the treatment stems from the concept of the propagation of discontinuities, the method of solution is somewhat different from the usual method of discontinuity analysis.

The equations of Naghdi [1] are employed in this thesis and we obtain a set of coupled displacement equations of motion for each case considered. Naghdi's equations are based on the Cosserat theory and include the effects of transverse shear, transverse normal stress and strain and rotatory inertia. Due to the presence of lower order derivatives, the governing displacement equations of motion are dispersive [2] causing the distortion of transient waves and the phase velocities of time harmonic waves to be frequency dependent. However, finite wave front speeds are assured due to the hyperbolic nature of these equations [3]. This is a primary requirement for solution by the method of discontinuity analysis.

The method of discontinuity analysis is well known and described in detail in [4], [5] and [6]. According to this method a wave is considered as a carrier of discontinuities in the field variable and/or its derivatives. The order of a wave is defined as the order of the lowest derivative of the field variable that is discontinuous across the wavefront. The discontinuities satisfy certain conditions across the wavefront from which it is possible to obtain a set of recursive relations known as transport-induction equations [5], [7]. These equations which govern the propagation of discontinuities, can be solved together with the specified time-dependent boundary condition to determine the discontinuities of all order at the wavefront. The transient solution is then represented in terms of a Taylor series expansion behind the wavefront, where the coefficients involved are the very discontinuities discussed above. Such expansions are suggested in the monographs of Achenbach [4] and Friedlander [8]. This method of solution will be known as the direct method.

Certain transient problems that we consider involve boundary loads that act for a finite time. For such cases the direct method if possible, will be tedious and it is preferable to adapt the Green's function concept. We define the unit pulse solution as the transient solution to the problem with a boundary condition involving the Heaviside unit function. This solution is easy to determine by the direct method and upon differentiation with respect to time gives the Green's function for the problem concerned [9]. The Green's function, together with the Duhamel integral, will yield the required transient solution [8].

The corresponding time harmonic problem can be solved by the Karal-Keller technique [10], where we formally assume asymptotic time harmonic series solutions to the equations of motion. The equations governing the variation of the coefficients in these series turn out to be exactly the transport-induction equations for the unit pulse problem. There is thus a one to one correspondence between the unit pulse problem and the corresponding time harmonic problem. For a given set of equations of motion it is much simpler to generate the transport-induction equations by the Karal-Keller technique than by the method of discontinuity analysis. This fact is first established and then exploited in this thesis.

In Chapter II the aim is twofold; viz to obtain the solutions to all the possible wave types in a plate and to establish the relationship between the unit pulse solution and the corresponding time harmonic solution. Earlier in this chapter the method of discontinuity analysis is described and applied to obtain the transport-induction equations necessary for a transient solution. To this end the field equations are cast into integral form in space-time allowing us to extract the form of the field equations when derivatives of the displacement are discontinuous [5]. The analysis yields a classification of the possible wave types in a plate together with their speeds and propagation conditions. For each wave type the transport-induction equations governing the propagation of an arbitrary order displacement discontinuity are obtained. These results are an extension to those presented by Cohen [11] who dealt with the geometric acoustics case, which is the value of the disturbance at the wavefront.

Later on in the same chapter, the Karal-Keller technique is used to obtain general steady state time-harmonic solutions to the plate equations. The coefficients in these series expansions are found to satisfy a set of recurrence relations from which we obtain the very same classification of the wave types. It is here that we establish the definite relationship that exists between the unit pulse solution and the corresponding time harmonic solution. The results obtained turn out to be in complete agreement with those of Kline and Kay [5] who considered the analogous problem for the electromagnetic field equations by a somewhat different approach.

In general the waves of the various types become coupled together in a fashion governed by the induction equations. We consider certain special types of wave motion in which there is no coupling between wave types and refer to these as pure wave motions. Some of these motions require constraining body forces or couples in order to be maintained. Finally in this chapter we consider the wave propagation problems corresponding to (i) a shear stress applied to a circular cavity in an unbounded plate, and (ii) a bending moment applied to a straight edge in an unbounded plate whose faces are constrained between two rigid plates. The results obtained are compared with existing closed form solutions [12], [13].

In Chapter III the propagation of axi-symmetric transients in shells of revolution with straight line generators is considered. The Karal-Keller technique is used, firstly to obtain the classification of the possible wave types together with their speeds and propagation conditions. The results so obtained are in agreement with those of Cohen [14] who proceeded along somewhat different lines. The transport-induction equations for the various wave types are then obtained. The prescribed boundary conditions together with the appropriate transport-induction equations can be used to obtain the solution to the given problem.

The series solutions obtained by our method are found to converge slowly, especially at large values of T, the time elapsed after the wavefront. The problem is similar as in the evaluation of the exponential of negative T using its Taylor series expansion, when T is large. Mainardi and Turchetti [15] used Padē approximants to accelerate the convergence of these series solutions. We present a simple numerical superposition technique as an alternative means of overcoming the same difficulty. The results obtained by using this technique agree with those of Mainardi and Turchetti who used Padé approximants.

Later on in the chapter we solve several numerical examples and discuss the results. The first example deals with the longitudinal impact of a conical shell. Herein we not only illustrate our technique of solution, but also verify them by comparing the results obtained with those obtained by using Laplace transforms [16]. The next two examples treat the propagation of axi-symmetric transients in a cylindrical shell due to velocity and acceleration boundary conditions. We also demonstrate how the response due to certain ground motions resulting from earthquake and blast loading may be obtained by incorporating the superposition technique. The effect of shell location and the effect of the thickness of a cylindrical shell on the response are next studied. Finally, in this chapter we discuss the approximate rod theories available for treating longitudinal transients in a cylinder.

The problem of general transient waves in cylindrical shells is treated in Chapter IV. The various displacement components are expressed in the form of Fourier series in θ (the circumferential coordinate) and the displacement equations of motion are written for each harmonic. The Karal-Keller technique is used as before to obtain the classification, speeds and propagation conditions of the possible wave types. Once again the results are in agreement with those obtained by Cohen [14]. Two of the possible wave types are coupled and as a result we obtain a coupled transport equation for these two waves and coupled induction equations for the other wave types. The prescribed boundary conditions, together with the transport-induction equations, can be used to obtain the solution to the given transient problem.

The approximate rod and beam theories available for treating transients in a cylinder are next discussed. This is followed by three numerical examples. In the first example the lateral impact of a cylinder is treated and the results obtained are compared with those obtained by using Laplace transforms [17]. The other two examples deal with the flexural and torsional problems pertaining to a cylindrical tank whose base is subjected to horizontal ground excitation. In the flexural problem we compare the solutions obtained by using the shell and beam theories. The effects of higher order waves induced due to homogeneous boundary conditions are illustrated and discussed in the first two examples.

CHAPTER II

TRANSIENT AND TIME HARMONIC WAVES IN PLATES

2.1 Equations of Motion

We consider the propagation of waves in linear, isotropic and homogeneous elastic plates. The plate equations that we utilize are those of linearised Cosserat plate theory as developed by Naghdi [1]. These equations developed from a *direct* two-dimensional approach are based on a director model and are equivalent to those developed from three-dimensional considerations, and include the effects of transverse shear deformation, transverse normal stress and strain and rotatory inertia. The displacement equations of motion separate into two sets governing the *extensional* and *bending* motions, respectively [11]. These are

$$\mu\nabla^2 \underset{\sim}{u} + (\lambda+\mu)\nabla(\nabla.\underset{\sim}{u}) + \lambda\nabla\delta^3 + \frac{\rho}{h}\underset{\sim}{F} = \frac{\rho}{h}\ddot{\underset{\sim}{u}} \quad , \tag{2.1}$$

$$\alpha_8\nabla^2\delta^3 - (\lambda+2\mu)h\delta^3 - \lambda(\nabla.\underset{\sim}{u})h + \rho L^3 = \rho\alpha\ddot{\delta}^3 \quad , \tag{2.2}$$

for the extensional theory, and

$$\nabla^2\underset{\sim}{\delta} + \frac{(3\lambda+2\mu)}{(\lambda+2\mu)}\nabla(\nabla.\underset{\sim}{\delta}) - \frac{\alpha_3}{\mu h\alpha}(\underset{\sim}{\delta}+\nabla u^3) + \frac{\rho}{\mu h\alpha}\underset{\sim}{L} = \frac{\rho}{\mu h}\ddot{\underset{\sim}{\delta}} \quad , \tag{2.3}$$

$$\nabla.\underset{\sim}{\delta} + \nabla^2 u^3 + \frac{\rho}{\alpha_3}F^3 = \frac{\rho}{\alpha_3}\ddot{u}^3 \quad , \tag{2.4}$$

for the bending theory.

In the above equations the displacement of the Cosserat plane is given by $\underset{\sim}{u}^* = (\underset{\sim}{u}, u^3)$ and the displacement of the director by $\underset{\sim}{\delta}^* = (\underset{\sim}{\delta}, \delta^3)$. The vectors $\underset{\sim}{u}, \underset{\sim}{\delta}$ represent the displacements parallel to the plane of the plate, while u^3, δ^3 represent the displacement normal to the plate. From the three-dimensional point of view, the assumed displacement $\underset{\sim}{U}^*$ across the plate space is given by [11],[1]

$$\underset{\sim}{U}^* = \underset{\sim}{u}^* + z\underset{\sim}{\delta}^* , \tag{2.5}$$

where z is the co-ordinate along the normal to the plate midsurface. ∇ is the two-dimensional gradient operator in the plane of the plate. Also λ, μ are Lame's constants, $\underset{\sim}{F}, F^3$ are body forces, $\underset{\sim}{L}, L^3$ are body couples, $\alpha = \frac{h^2}{12}$, while the constitutive coefficients α_3 and α_8 are taken as constants and could take on values depending on the problem at hand [11],[1]. The mass per unit area is ρ while h is the plate thickness.

The plate equations (2.1) - (2.4) being hyperbolic, ensure finite wave front velocities for the propagation of disturbances [2]. In this respect they are similar to the equations of motion in three-dimensional elasticity and are suitable for studying the dynamic response in plates. However due to the presence of terms of lower order differentiation, these plate equations are *dispersive* [3]. Thus a pulse will suffer distortion and the phase velocity of a harmonic wavetrain will depend on the frequency ω.

Introducing the notations

$$\underset{\sim}{w}_1 = (\underset{\sim}{u}, \delta^3),\ \underset{\sim}{w}_2 = (\underset{\sim}{\delta}, u^3),\ \underset{\sim}{f}_1 = -(\underset{\sim}{F}, L^3),\ \underset{\sim}{f}_2 = -(\underset{\sim}{L}, F^3) \quad , \qquad (2.6)$$

equations (2.1) - (2.4) can be conveniently written as

$$\underset{\sim}{L}_\alpha \underset{\sim}{w}_\alpha = \rho \underset{\sim}{f}_\alpha \ , \ \alpha = 1,2 \quad , \qquad (2.7)$$

where $\underset{\sim}{L}_\alpha$ is a suitably defined linear second order differential operator.

2.2 Transient Waves and Discontinuities

Consider a source of disturbance acting over some curve in a homogeneous isotropic elastic plate as shown in Figure 1a.[1] If the source begins to act at time t = 0, then for t>0 this disturbance will spread into the plate with a constant wave front velocity G. The wave front will constitute a family of parallel curves $\psi(x,y) = Gt$ in the x,y plane of the plate while sweeping out a hypercone $\phi(x,y,t) = 0$ in space-time. The value of the field at a point $P_0(x_0, y_0, t_0)$ on the wave front is called the *geometrical acoustic* field by analogy to the geometrical optics situation arising in [5].

---

[1] The results to follow are readily generalized to nonhomogeneous plates. The general features of the analysis are analogous to those presented here. The complication appears as an algebraic one, due to the fact that the speed of propagation is no longer constant.

The value of this field at any point $P(x_o, y_o, t)$, $t > t_o$, behind the wave front will constitute the so-called *transient* or *pulse* solution to the disturbance problem.

We assume a transient solution to equation (2.7) in the form of a Taylor's series expansion [4],[8] at the wave front into the region behind it. Thus we write

$$\underset{\sim}{w}_\alpha = \sum_{n=o}^{\infty} \underset{\sim}{[}\frac{\partial^n \underset{\sim}{w}_\alpha}{\partial t^n}\underset{\sim}{]}_{t=t_o} \frac{\langle t-t_o \rangle^n}{n!} \quad , \tag{2.8}$$

where $\langle , \rangle = 0$ if the argument is negative while $\underset{\sim}{[}\ \underset{\sim}{]}$ indicates the *discontinuity* or *jump* of the argument across the wave front. These discontinuities occur at the wave front since the region ahead of the wave is undisturbed. The wave is thus naturally a carrier of discontinuities. The lowest order derivative of $\underset{\sim}{w}_\alpha$ having a discontinuity defines the order of the wave. A first order wave is called a shock or strain wave and waves of this type will constitute the subject matter dealt with herein. Higher order waves yield results which are completely analogous to those for first order waves. For first order waves, a knowledge of the first order discontinuities on the wave front will constitute the geometric acoustics solution, while a knowledge of the higher order discontinuities will allow calculation of the transient solution from equation (2.8).

Associated with the geometry of the wave front at any point are its unit tangent $\underset{\sim}{\lambda}$ and unit normal $\underset{\sim}{\nu}$. We use ℓ and s to denote arc lengths along the wave curve, and perpendicular to it, respectively. Thus s measures distance along the rays defined as the orthogonal trajectories to the wave curves, which for homogeneous isotropic plates are straight lines. We find it convenient to define the vector differential operator ∇_D by

$$\nabla_D = \nabla + \frac{\underset{\sim}{\nu}}{G}\frac{\partial}{\partial t} \quad . \tag{2.9}$$

This operator allows calculation of all one-sided directional derivatives along the wave surface $\phi(x,y,t) = 0$. In particular the operator $\frac{D}{Dt}$ is defined by

$$\frac{D}{Dt} = G\underset{\sim}{\nu}.\nabla_D = \frac{\partial}{\partial t} + G\underset{\sim}{\nu}.\nabla \quad . \tag{2.10}$$

This is the so-called *displacement* derivative [7] and calculates rate of change as seen by an observer moving along the rays with the wave speed G, i.e. moving with the wave front. Applying equation (2.10) to the wave surface equation $\phi(x,y,t) = \psi(x,y) - Gt = 0$, we compute that

$$\underset{\sim}{\nu} = \nabla\phi = \nabla\psi \;, \; \kappa = -\nabla^2\psi \quad , \tag{2.11}$$

where κ is the curvature of the wave front.

In terms of the operator ∇_D the so-called Hadamard's Lemma [7] takes the form

$$\underset{\sim}{[}\nabla_D \underset{\sim}{w}_{\alpha}\underset{\sim}{]} = \nabla_D \underset{\sim}{[}\underset{\sim}{w}_{\alpha}\underset{\sim}{]} \quad . \tag{2.12}$$

In what is to follow it is convenient to represent vector quantities in terms of components tangent and normal to the wave front. Thus we write

$$\underset{\sim}{w}_{\alpha} = w^{\lambda}_{\alpha}\underset{\sim}{\lambda} + w^{\nu}_{\alpha}\underset{\sim}{\nu} \quad , \tag{2.13}$$

and moreover define the directional derivatives

$$\frac{d}{d\ell} = \underset{\sim}{\lambda}\cdot\nabla \quad , \quad \frac{d}{ds} = \underset{\sim}{\nu}\cdot\nabla \quad . \tag{2.14}$$

In particular we obtain from equations (2.12), (2.9) and $(2.14)_2$ the compatibility relations

$$[\underset{\sim}{w}_{\alpha,n+1}] = -\underset{\sim}{G}\left[\frac{d\underset{\sim}{w}_{\alpha,n}}{ds}\right] + \frac{D}{Dt}[\underset{\sim}{w}_{\alpha,n}] \quad , \quad n \geq 0 \quad , \tag{2.15}$$

where the comma followed by the subscript n indicates an n^{th} order time derivative.

In order to determine the possible types of discontinuities and their behaviour at the wave front we must utilize the field equations (2.7) to obtain the appropriate governing discontinuity equations. Since we are dealing with first order waves we shall require discontinuity equations of a lower order than can be obtained by taking the jumps of an nth order $(n \geq 0)$ time derivative of equation (2.7). These lower order equations are obtained by following the procedure utilised in [5] to deal with Maxwell's equations. We introduce a *testing* function Ω, which possesses derivatives of all order. The testing function and its derivatives vanish on and outside the boundary ∂R of a domain R in space-time. Multiplying the extensional field equation (2.1) and (2.2) by Ω, integrating over R and utilising integration by parts we obtain

$$\int_R \{\mu(\nabla\Omega.\nabla)\underset{\sim}{u}+(\lambda+\mu)\nabla\Omega(\nabla.\underset{\sim}{u})+\lambda\nabla\Omega\delta^3-\frac{\rho}{h}\dot{\Omega}\dot{\underset{\sim}{u}}-\Omega\frac{\rho}{h}\underset{\sim}{F}\} = 0 \quad , \qquad (2.16)$$

$$\int_R \{\alpha_8(\nabla\Omega.\nabla)\delta^3+(\lambda+2\mu)h\Omega\delta^3-\lambda(\nabla\Omega.\underset{\sim}{u})h-\rho\alpha\dot{\Omega}\dot{\delta}^3-\Omega\rho L^3\} = 0 \,. \qquad (2.17)$$

Equations (2.16) and (2.17) are integral forms of the field equations (2.1) and (2.2) respectively, and these are mathematically equivalent to one another in regions where the derivatives involved are continuous. We also define $\dot{u} = u_{,1}$ etc.

We now assume the surface of discontinuity $\phi(x,y,t) = 0$ to pass through the region R, dividing it into regions R_1 and R_2 as in Figure 1b. Reversing the procedure used to obtain equations (2.16) and (2.17) with appropriate integration by parts over the domains R_1 and R_2, inside of which the necessary derivatives are continuous, we find[2]

$$\underset{\sim}{\mu}[(\nabla\phi.\nabla)\underset{\sim}{u}] + (\lambda+\mu)\nabla\phi[\underset{\sim}{\nabla}.\underset{\sim}{u}] + \lambda\nabla\phi[\underset{\sim}{\delta^3}] + \frac{\rho}{h}G[\dot{\underset{\sim}{u}}] = 0 \qquad (2.18)$$

---

[2] In this analysis we assume that the body forces $\underset{\sim}{f}_\alpha$ are C^∞ and note that the continuity of $\underset{\sim}{f}_\alpha$ has been used in obtaining (2.18) and (2.19)

$$\underset{\sim}{\alpha_8[}(\nabla\phi.\nabla)\delta^3\underset{\sim}{]} - \lambda h\underset{\sim}{[}\nabla\phi.\underset{\sim}{u}\underset{\sim}{]} + \rho\alpha G\underset{\sim}{[}\dot{\delta}^3\underset{\sim}{]} = 0 \ . \tag{2.19}$$

Equations (2.18) and (2.19) are the required discontinuity equations and are a consequence of the field equations (2.1) and (2.2) at a surface of discontinuity. In an analogous fashion, the plate bending equations (2.3) and (2.4) lead to the discontinuity equations.

$$\underset{\sim}{[}(\nabla\phi.\nabla)\underset{\sim}{\delta}\underset{\sim}{]} + \frac{(3\lambda+2\mu)}{(\lambda+2\mu)}\nabla\phi\underset{\sim}{[}\nabla.\underset{\sim}{\delta}\underset{\sim}{]} - \frac{\alpha_3}{\mu h\alpha}\nabla\phi\underset{\sim}{[}u^3\underset{\sim}{]} + \frac{\rho}{\mu h}G\underset{\sim}{[}\dot{\underset{\sim}{\delta}}\underset{\sim}{]} = 0 \ , \tag{2.20}$$

$$\underset{\sim}{[}\nabla\phi.\underset{\sim}{\delta}\underset{\sim}{]} + \underset{\sim}{[}(\nabla\phi.\nabla)u^3\underset{\sim}{]} + \frac{\rho}{\alpha_3}G\underset{\sim}{[}\dot{u}^3\underset{\sim}{]} = 0 \ . \tag{2.21}$$

In order to obtain discontinuity equations of higher order, i.e. governing jumps in higher order derivatives, we need only take the jumps of any n^{th} order $(n\geq 0)$ time derivative of equation (2.7). This leads to

$$\begin{aligned}\mu\underset{\sim}{[}(\underset{\sim}{\nu}.\nabla)\underset{\sim}{u},_{n}\underset{\sim}{]} + (\lambda+\mu)\underset{\sim}{\nu}\underset{\sim}{[}\nabla.\underset{\sim}{u},_{n}\underset{\sim}{]} + \lambda\underset{\sim}{\nu}\underset{\sim}{[}\delta^3,_{n}\underset{\sim}{]} + G\frac{\rho}{h}\underset{\sim}{[}\underset{\sim}{u},_{n+1}\underset{\sim}{]} \\ = G\{\mu\nabla_D.\underset{\sim}{[}\nabla\underset{\sim}{u},_{n-1}\underset{\sim}{]} + (\lambda+\mu)\ \nabla_D\underset{\sim}{[}\nabla.\underset{\sim}{u},_{n-1}\underset{\sim}{]} + \lambda\nabla_D\underset{\sim}{[}\delta^3,_{n-1}\underset{\sim}{]}\} \ ,\end{aligned} \tag{2.22}$$

$$\begin{aligned}\alpha_8\underset{\sim}{[}(\underset{\sim}{\nu}.\nabla)\delta^3,_{n}\underset{\sim}{]} - \lambda h\underset{\sim}{[}\underset{\sim}{\nu}.\underset{\sim}{u},_{n}\underset{\sim}{]} + G\rho\alpha\underset{\sim}{[}\delta^3,_{n+1}\underset{\sim}{]} \\ = G\{\alpha_8\nabla_D.\underset{\sim}{[}\nabla\delta^3,_{n-1}] - (\lambda+2\mu)h\underset{\sim}{[}\delta^3,_{n-1}\underset{\sim}{]} - \lambda h\nabla_D.\underset{\sim}{[}\underset{\sim}{u},_{n-1}\underset{\sim}{]}\} \ ,\end{aligned} \tag{2.23}$$

for the extensional theory, and

$$\begin{aligned}\underset{\sim}{[}(\underset{\sim}{\nu}.\nabla)\underset{\sim}{\delta},_{n}\underset{\sim}{]} + \frac{(3\lambda+2\mu)}{(\lambda+2\mu)}\underset{\sim}{\nu}\underset{\sim}{[}\nabla.\underset{\sim}{\delta},_{n}\underset{\sim}{]} + \frac{\alpha_3}{\mu h\alpha}\underset{\sim}{\nu}\underset{\sim}{[}u^3,_{n}\underset{\sim}{]} + \frac{G\rho}{\mu h\alpha}\underset{\sim}{[}\underset{\sim}{\delta},_{n+1}\underset{\sim}{]} \\ = G\{\nabla_D.\underset{\sim}{[}\nabla\underset{\sim}{\delta},_{n-1}\underset{\sim}{]} + \frac{(3\lambda+2\mu)}{(\lambda+2\mu)}\nabla_D\underset{\sim}{[}\nabla.\underset{\sim}{\delta},_{n-1}\underset{\sim}{]} - \frac{\alpha_3}{\mu h\alpha}\underset{\sim}{[}\underset{\sim}{\delta},_{n-1}\underset{\sim}{]} - \frac{\alpha_3}{\mu h\alpha}\nabla_D\underset{\sim}{[}u^3,_{n-1}\underset{\sim}{]}\} \ ,\end{aligned} \tag{2.24}$$

$$[\underset{\sim}{\nu}\cdot\underset{\sim}{\delta},_n]+[(\underset{\sim}{\nu}\cdot\nabla)u^3,_n]+\frac{\rho G}{\alpha_3}[u^3,_{n+1}] = G\{\nabla_D\cdot[\underset{\sim}{\delta},_{n-1}]+\nabla_D\cdot[\nabla u^3,_{n-1}]\} , \tag{2.25}$$

for the bending theory. We note that in writing equations (2.22) - (2.25) we have modified their forms by use of equation (2.9).

I *Extensional Waves*

We now turn our attention to the consequences of the above discontinuity equations for the case of extensional waves. Equations (2.18) and (2.19) determine the *propagation conditions* for extensional waves. These conditions determine the possible types of waves which can propagate, as well as their associated speeds of propagation. If we take the scalar product of equation (2.18) with $\underset{\sim}{\lambda}$ and $\underset{\sim}{\nu}$, utilise equation (2.13) as well as the appropriate first order compatibility relation obtained from equation (2.15) by putting n = 0 and $[\underset{\sim}{w}_1] = 0$, we find from equations (2.18) and (2.19) that

$$(G_T^2-G^2)[u^{\lambda},_1] = 0, \quad (G_L^2-G^2)[u^{\nu},_1] = 0, \quad (G_S^2-G^2)[\delta^3,_1] = 0, \tag{2.26}$$

where

$$G_T^2 = \frac{\mu h}{\rho} , \quad G_L^2 = \frac{(\lambda+2\mu)h}{\rho} , \quad G_S^2 = \frac{\alpha_8}{\rho\alpha} , \tag{2.27}$$

Equations (2.26) will define the three types of waves. For each of these, if the values of the possible jumps are given on an initial curve, their variations as they move with the wave front will be governed by equations (2.22) and (2.23).

If we take the scalar product of equation (2.22) with $\underset{\sim}{\lambda}$ and $\underset{\sim}{\nu}$, use equations (2.12)-(2.15), we obtain as a consequence of equations (2.22) and (2.23), a system of three first order differential equations which involve jumps of order n,(n-1) and (n-2) in the field quantities. These equations determine the *transport-induction* equations for each type of wave by substitution of the appropriate solution to equations (2.26) into them. We now proceed to give a classification of the wave types along with their transport-induction equations.

(i) *Longitudinal Wave*

$$[u^{\nu}_{,1}] \neq 0 \ , \quad [u^{\lambda}_{,1}] = [\delta^{3}_{,1}] = 0 \ , \quad G^2 = G_L^2 \ , \tag{2.28}$$

$$\begin{aligned} 2\frac{d}{ds}[u^{\nu}_{,n}] - \kappa[u^{\nu}_{,n}] &= -\frac{1}{2(1-\nu)}\left\{\frac{d}{d\ell}[u^{\lambda}_{,n}] - G_L \frac{d}{ds}(\nabla\cdot[\underset{\sim}{u}_{,n-1}])\right\} \\ &- \frac{\nu}{(1-\nu)}\left([\delta^{3}_{,n}] - G_L \frac{d}{ds}[\delta^{3}_{,n-1}]\right) + \frac{G_T^2}{G_L}\underset{\sim}{\nu}\cdot\nabla^2[\underset{\sim}{u}_{,n-1}] \ , \end{aligned} \tag{2.29}$$

$$\begin{aligned} [u^{\lambda}_{,n}] &= -(1-2\nu)G_L\left(2\frac{d}{ds}[u^{\lambda}_{,n-1}] - \kappa[u^{\lambda}_{,n-1}] - G_L\underset{\sim}{\lambda}\cdot\nabla^2[\underset{\sim}{u}_{,n-2}]\right) \\ &+ G_L \frac{d}{d\ell}\left(G_L \nabla\cdot[\underset{\sim}{u}_{,n-2}] + 2\nu G_L[\delta^{3}_{,n-2}] - [u^{\nu}_{,n-1}]\right) \ , \end{aligned} \tag{2.30}$$

$$\begin{aligned} (G_L^2 - G_S^2)[\delta^{3}_{,n}] &= \frac{2\nu}{(1-2\nu)}\cdot\frac{G_T^2 G_L}{\alpha}\left([u^{\nu}_{,n-1}] - G_L\nabla\cdot[\underset{\sim}{u}_{,n-2}]\right) - \\ & G_L G_S^2\left(2\frac{d}{ds}[\delta^{3}_{,n-1}] - \kappa[\delta^{3}_{,n-1}]\right) + G_L^2 G_S^2 \nabla^2[\delta^{3}_{,n-1}] - \frac{G_L^4}{\alpha}[\delta^{3}_{,n-2}] \ . \end{aligned} \tag{2.31}$$

(ii) *Shear Wave*

$$[u^{\lambda}_{,1}] \neq 0 \ , \quad [u^{\nu}_{,1}] = [\delta^{3}_{,1}] = 0 \ , \quad G^2 = G_T^2 \ , \tag{2.32}$$

$$2\frac{d}{ds}[u^{\lambda}_{,n}] - \kappa[u^{\lambda}_{,n}] = -\frac{1}{(1-2\nu)}\frac{d}{d\ell}\left([u^{\nu}_{,n}] - G_T(\nabla\cdot[\underset{\sim\sim}{u}_{,n-1}])\right.$$

$$\left.-2\nu G_T[\delta^3_{,n-1}]\right) - G_T\lambda\cdot\nabla^2[\underset{\sim\sim}{u}_{,n-1}] \quad , \tag{2.33}$$

$$[u^{\nu}_{,n}] = G_T\frac{d}{d\ell}[u^{\lambda}_{,n-1}] + 2(1-\nu)G_T\left(2\frac{d}{ds}[u^{\nu}_{,n-1}] - \kappa[u^{\nu}_{,n-1}]\right)$$

$$-(1-2\nu)G_T^2\nu\cdot\nabla^2[\underset{\sim\sim}{u}_{,n-2}] + 2\nu G_T\left([\delta^3_{,n-1}] - G_T\frac{d}{ds}[\delta^3_{,n-2}]\right) - G_T^2\frac{d}{ds}(\nabla\cdot[\underset{\sim\sim}{u}_{,n-2}]) \; , \tag{2.34}$$

$$(G_T^2-G_S^2)[\delta^3_{,n}] = \frac{2\nu}{(1-2\nu)}\frac{G_T^3}{\alpha}\left([u^{\nu}_{,n-1}] - G_T\nabla\cdot[\underset{\sim\sim}{u}_{,n-2}]\right) - G_TG_S^2\left(2\frac{d}{ds}[\delta^3_{,n-1}]\right.$$

$$\left.-\kappa[\delta^3_{,n-1}]\right) + G_T^2G_S^2\nabla^2[\delta^3_{,n-2}] - \frac{G_T^2G_L^2}{\alpha}[\delta^3_{,n-2}] \; . \tag{2.35}$$

(iii) *Squeeze-gradient wave*

$$[\delta^3_{,1}] \neq 0 \; , \; [\underset{\sim\sim}{u}_{,1}] = 0 \; , \; G^2 = G_S^2 \quad , \tag{2.36}$$

$$2\frac{d}{ds}[\delta^3_{,n}] - \kappa[\delta^3_{,n}] = \frac{2\nu}{(1-2\nu)}\frac{G_T^2}{\alpha G_S^2}\left([u^{\nu}_{,n}] - G_S\nabla\cdot[\underset{\sim\sim}{u}_{,n-1}]\right)$$

$$+ G_S\nabla^2[\delta^3_{,n-1}] - \frac{G_L^2}{\alpha G_S^2}[\delta^3_{,n-1}] \quad , \tag{2.37}$$

$$(G_L^2-G_S^2)[u^{\nu}_{,n}] = G_L^2G_S\left(2\frac{d}{ds}[u^{\nu}_{,n-1}] - \kappa[u^{\nu}_{,n-1}]\right) - G_T^2G_S^2\nu\cdot\nabla^2[\underset{\sim\sim}{u}_{,n-2}]$$

$$+ \frac{G_S}{2(1-\nu)}\left\{G_L^2\frac{d}{d\ell}[u^{\lambda}_{,n-1}] - G_L^2G_S\frac{d}{ds}(\nabla\cdot[\underset{\sim\sim}{u}_{,n-2}])\right\} \tag{2.38}$$

$$+\frac{2\nu}{(1-2\nu)}G_T^2G_S\left([\delta^3_{,n-1}] - G_S\frac{d}{ds}[\delta^3_{,n-2}]\right) \; ,$$

$$(G_T^2-G_S^2)[\underset{\sim}{u},{}^{\lambda}_{n}] = G_T^2G_S\left(2\frac{d}{ds}[\underset{\sim}{u},{}^{\lambda}_{n-1}]-\kappa[\underset{\sim}{u},{}^{\lambda}_{n-1}]-G_S\underset{\sim}{\lambda}\cdot\nabla^2[\underset{\sim\sim}{u},_{n-2}]\right)$$

$$+\frac{G_S}{2(1-\nu)}\frac{d}{d\ell}\left(G_L^2[\underset{\sim}{u},{}^{\nu}_{n-1}]-G_L^2G_S(\nabla\cdot[\underset{\sim\sim}{u},_{n-2}])\right)-\frac{2\nu}{(1-2\nu)}G_T^2G_S^2[\underset{\sim}{\delta},{}^{3}_{n-2}]) . \tag{2.39}$$

We have written the above equations in terms of the Poisson's ratio ν and we note that $n \geq 1$ in them. Moreover we add that in obtaining the above equations we have used $t = \psi(x,y)G^{-1}$ to eliminate explicit dependence on time at the wave front. Equations (2.29), (2.33) and (2.37) are the transport or *decay* equations and determine the variation in the quantities $[\underset{\sim}{u},{}^{\nu}_{n}]$, $[\underset{\sim}{u},{}^{\lambda}_{n}]$ and $[\underset{\sim}{\delta},{}^{3}_{n}]$, respectively, for the three types of waves, provided these are specified on an initial wave curve. The role played by the pairs of equations following the decay equation in each case is to determine the higher order discontinuities induced by those of lower order. Moreover, they bring into play the coupling of wave types that will occur for the discontinuities of order greater than one.

II *Bending Waves*

For the case of bending waves, the analysis is entirely analogous to that of extensional waves. In this case we utilise equations (2.20), (2.21) to obtain the propagation conditions and equations (2.24), (2.25) to obtain the transport-induction equations. We now present the classification and transport-induction equations for the three types of bending waves.

(i) *Bending wave*

$$\underset{\sim}{[\delta^{\nu}{}_{,1}]} \neq 0 \;, \quad \underset{\sim}{[\delta^{\lambda}{}_{,1}]} = \underset{\sim}{[u^{3}{}_{,1}]} = 0 \;, \quad G^{2} = G_{B}^{2} \;, \tag{2.40}$$

$$\begin{aligned} 2\frac{d}{ds}\underset{\sim}{[\delta^{\nu}{}_{,n}]} - \kappa\underset{\sim}{[\delta^{\nu}{}_{,n}]} = & -\frac{(1+\nu)}{2}\left\{\frac{d}{d\ell}\underset{\sim}{[\delta^{\lambda}{}_{,n}]} - G_{B}\frac{d}{ds}(\nabla\cdot\underset{\sim\sim}{[\delta}{}_{,n-1}])\right\} \\ & -\frac{G_{K}^{2}}{\alpha G_{B}^{2}}\underset{\sim}{[u^{3}{}_{,n}]} + \frac{G_{T}^{2}}{G_{B}}\underset{\sim}{\nu}\cdot\nabla^{2}\underset{\sim\sim}{[\delta}{}_{,n-1}] - \frac{G_{K}^{2}}{\alpha G_{B}}\left(\underset{\sim}{[\delta^{\nu}{}_{,n-1}]} + \frac{d}{ds}\underset{\sim}{[u^{3}{}_{,n-1}]}\right), \end{aligned} \tag{2.41}$$

$$\begin{aligned} (G_{B}^{2}-G_{T}^{2})\underset{\sim}{[\delta^{\lambda}{}_{,n}]} = & -G_{B}G_{T}^{2}\left(2\frac{d}{ds}\underset{\sim}{[\delta^{\lambda}{}_{,n-1}]} - \kappa\underset{\sim}{[\delta^{\lambda}{}_{,n-1}]}\right) + G_{B}^{2}G_{T}^{2}\underset{\sim}{\lambda}\cdot\nabla^{2}\underset{\sim\sim}{[\delta}{}_{,n-2}] \\ & -\frac{(1+\nu)}{(1-\nu)}G_{B}G_{T}^{2}\frac{d}{d\ell}\left(\underset{\sim}{[\delta^{\nu}{}_{,n-1}]} - G_{B}\nabla\cdot\underset{\sim\sim}{[\delta}{}_{,n-2}]\right) - \frac{G_{B}^{2}G_{K}^{2}}{\alpha}\left(\underset{\sim}{[\delta^{\lambda}{}_{,n-2}]} + \frac{d}{d\ell}\underset{\sim}{[u^{3}{}_{,n-2}]}\right), \end{aligned} \tag{2.42}$$

$$\begin{aligned} (G_{B}^{2}-G_{K}^{2})\underset{\sim}{[u^{3}{}_{,n}]} = & -G_{B}G_{K}^{2}\left(2\frac{d}{ds}\underset{\sim}{[u^{3}{}_{,n-1}]} - \kappa\underset{\sim}{[u^{3}{}_{,n-1}]} + \underset{\sim}{[\delta^{\nu}{}_{,n-1}]}\right) \\ & + G_{B}^{2}G_{K}^{2}\left(\nabla\cdot\underset{\sim\sim}{[\delta}{}_{,n-2}] + \nabla^{2}\underset{\sim}{[u^{3}{}_{,n-2}]}\right) . \end{aligned} \tag{2.43}$$

(ii) *Twisting wave*

$$\underset{\sim}{[\delta^{\lambda}{}_{,1}]} \neq 0 \;, \quad \underset{\sim}{[\delta^{\nu}{}_{,1}]} = \underset{\sim}{[u^{3}{}_{,1}]} = 0 \;, \quad G^{2} = G_{T}^{2} \;, \tag{2.44}$$

$$\begin{aligned} 2\frac{d}{ds}\underset{\sim}{[\delta^{\lambda}{}_{,n}]} - \kappa\underset{\sim}{[\delta^{\lambda}{}_{,n}]} = & -\frac{(1+\nu)}{(1-\nu)}\frac{d}{d\ell}\left(\underset{\sim}{[\delta^{\nu}{}_{,n}]} - G_{B}\nabla\cdot\underset{\sim\sim}{[\delta}{}_{,n-1}]\right) \\ & + G_{T}\underset{\sim}{\lambda}\cdot\nabla^{2}\underset{\sim\sim}{[\delta}{}_{,n-1}] - \frac{G_{K}^{2}}{\alpha G_{T}}\left(\underset{\sim}{[\delta^{\lambda}{}_{,n-1}]} + \frac{d}{d\ell}\underset{\sim}{[u^{3}{}_{,n-1}]}\right) , \end{aligned} \tag{2.45}$$

$$(G_B^2-G_T^2)\,\underset{\sim}{[\delta^\nu,_n]} = G_B^2 G_T \left(2\frac{d}{ds}\underset{\sim}{[\delta^\nu,_{n-1}]}-\kappa\,\underset{\sim}{[\delta^\nu,_{n-1}]}\right) + \frac{G_T G_K^2}{\alpha}\underset{\sim}{[u^3,_{n-1}]}$$

$$+\ \frac{(1+\nu)}{(1-\nu)}G_T^3\left\{\frac{d}{d\ell}\underset{\sim}{[\delta^\lambda,_{n-1}]}-G_T\frac{d}{ds}(\nabla\cdot\underset{\approx}{[\delta},_{n-2}])\right\}-G_T^4\underset{\sim}{\nu}\cdot\nabla^2\underset{\approx}{[\delta},_{n-2}] \qquad (2.46)$$

$$+\ \frac{G_T^2G_K^2}{\alpha}\left(\underset{\sim}{[\delta^\nu,_{n-2}]}+\frac{d}{ds}\underset{\sim}{[u^3,_{n-2}]}\right) \quad ,$$

$$(G_T^2-G_K^2)\,\underset{\sim}{[u^3,_n]} = -G_T G_K^2\left(2\frac{d}{ds}\underset{\sim}{[u^3,_{n-1}]}-\kappa\,\underset{\sim}{[u^3,_{n-1}]}\right)-G_T G_K^2\underset{\sim}{[\delta^\nu,_{n-1}]}$$

$$(2.47)$$

$$+\ G_T^2G_K^2\left(\nabla\cdot\underset{\approx}{[\delta},_{n-2}]+\nabla^2\underset{\sim}{[u^3,_{n-2}]}\right) \quad .$$

(iii) *Kink wave*

$$\underset{\sim}{[u^3,_1]}\neq 0\ ,\quad \underset{\approx}{[\delta},_1]=0\ ,\quad G^2=G_K^2\ , \qquad (2.48)$$

$$2\frac{d}{ds}\underset{\sim}{[u^3,_n]}-\kappa\,\underset{\sim}{[u^3,_n]} = -\underset{\sim}{[\delta^\nu,_n]}+G_K\nabla\cdot\underset{\approx}{[\delta},_{n-1}]+G_K\nabla^2\underset{\sim}{[u^3,_{n-1}]}, \qquad (2.49)$$

$$(G_B^2-G_K^2)\,\underset{\sim}{[\delta^\nu,_n]} = G_K G_B^2\left(2\frac{d}{ds}\underset{\sim}{[\delta^\nu,_{n-1}]}-\kappa\,\underset{\sim}{[\delta^\nu,_{n-1}]}\right)$$

$$+\ \frac{(1+\nu)}{(1-\nu)}G_K G_T^2\left\{\frac{d}{d\ell}[\delta^\lambda,_{n-1}]-G_K\frac{d}{ds}(\nabla\cdot\underset{\approx}{[\delta},_{n-2}])\right\}-G_K^2G_T^2\underset{\sim}{\nu}\cdot\nabla^2\underset{\approx}{[\delta},_{n-2}]$$

$$+\ \frac{G_K^3}{\alpha}\left(G_K\underset{\sim}{[\delta^\nu,_{n-2}]}+G_K\frac{d}{ds}\underset{\sim}{[u^3,_{n-2}]}-\underset{\sim}{[u^3,_{n-1}]}\right) \quad , \qquad (2.50)$$

$$(G_T^2-G_K^2)\,\underset{\sim}{[\delta^\lambda,_n]} = G_K G_T^2\left(2\frac{d}{ds}\underset{\sim}{[\delta^\lambda,_{n-1}]}-\kappa\,\underset{\sim}{[\delta^\lambda,_{n-1}]}\right)+G_K^2G_T^2\underset{\sim}{\lambda}\cdot\nabla^2\underset{\sim}{[\delta},_{n-2}]$$

$$+\ \frac{(1+\nu)}{(1-\nu)}G_K G_T^2\frac{d}{d\ell}\left(\underset{\sim}{[\delta^\nu,_{n-1}]}-G_K\nabla\cdot\underset{\approx}{[\delta},_{n-2}]\right)-\frac{G_K^4}{\alpha}\left(\underset{\sim}{[\delta^\lambda,_{n-2}]}+\frac{d}{d\ell}\underset{\sim}{[u^3,_{n-2}]}\right).$$

$$(2.51)$$

In equations (2.40)-(2.51) we have set

$$G_B^2 = \frac{4(\lambda+\mu)\mu h}{(\lambda+2\mu)\rho} , \quad G_T^2 = \frac{\mu h}{\rho} , \quad G_K^2 = \frac{\alpha_3}{\rho} . \tag{2.52}$$

The above results for both the extensional and bending waves are generalisations of those obtained by Cohen in [11]. We remark that the procedure used here to obtain the propagation conditions is an alternative to that utilised in [11].

We note finally that the transport equations for all of the above types of waves are of the form

$$2\frac{d}{ds}[\underset{\sim}{w},_{n}] - \kappa[\underset{\sim}{w},_{n}] = G\, F_{n-1} , \quad n \geq 1 . \tag{2.53}$$

This equation has the solution [10]

$$[\underset{\sim}{w},_{n}] = [\underset{\sim}{w},_{no}]\left(\frac{\kappa}{\kappa_o}\right)^{\frac{1}{2}} + \frac{G}{2}\kappa^{\frac{1}{2}}\int_{s_o}^{s}(\kappa(\tau))^{-\frac{1}{2}}F_{n-1}(\tau)d\tau , \tag{2.54}$$

where the subscript o indicates evaluation at the initial wave-curve.

2.3 Steady State Time Harmonic Waves

Cohen in [11] examined the question of steady state time harmonic *plane* wave solutions of the plate equations (2.7) in the absence of body forces, i.e. with $\underset{\sim}{f}_\alpha = 0$. For waves of this type the possible phase velocities $V = \omega k^{-1}$, where ω is the frequency and k the wave number, were found as a function of wave number. It was found that with the exception of one mode of propagation in the case of extensional waves, that all other wave types were dispersive. In the limiting case of infinite frequency or wave number, all phase velocities reduced to the corresponding speeds of propagation of pulses found in section 2.2 of this chapter. Here we seek harmonic wave solutions of a more general nature than those in [11], corresponding to waves which are generally curved and which arise as a consequence of a time harmonic disturbance applied to an arbitrary curve in the plane of the plate.

Thus we begin by assuming an asymptotic series for the displacements in the form

$$\underset{\sim}{w}_\alpha = e^{i\omega(S-t)} \sum_{n=o}^{\infty} \frac{\underset{\sim}{A}_{\alpha n}}{(i\omega)^n} \quad , \tag{2.55}$$

which is to represent the steady state behaviour of the plate for large frequencies. Series of this type were introduced in [10], where S is called the *phase* function, to investigate steady state time harmonic behaviour in an unbounded three-dimensional elastic non-dispersive medium. For high frequencies the first term in the series predominates and we may regard this as an approximation to the solution. For other frequencies the higher order terms in the series may be viewed as corrections to the disturbance arising due to (a) the dispersive nature of the governing equations, (b) the geometry of the wave being non-planar, and (c) the variation of amplitude over the wave.

On substituting equation (2.55) into equation (2.1) and (2.2) with $\underset{\sim}{f}_1 = \underset{\sim}{0}$, setting $\underset{\sim}{A}_{1n} = (\underset{\sim}{A}_n, A_n^3)$ and formally requiring that the coefficients of powers of $(i\omega)$ separately vanish, we obtain the recurrence relations for $n \geq 1$ as

$$
\begin{aligned}
&\underset{\sim}{A}_n\{\mu(\nabla s)^2-\rho h^{-1}\} + (\lambda+\mu)\nabla s(\underset{\sim}{A}_n.\nabla s) + 2\mu(\nabla s.\nabla)\underset{\sim}{A}_{n-1} + \mu\nabla^2 s\ \underset{\sim}{A}_{n-1} \\
&+ (\lambda+\mu)\nabla s(\nabla.\underset{\sim}{A}_{n-1}) + (\lambda+\mu)\nabla(\underset{\sim}{A}_{n-1}.\nabla s) + \lambda\nabla s\ A^3_{n-1} \qquad (2.56) \\
&+ \mu\nabla^2\underset{\sim}{A}_{n-2} + (\lambda+\mu)\nabla(\nabla.\underset{\sim}{A}_{n-2}) + \lambda\nabla A^3_{n-2} = 0 \quad ,
\end{aligned}
$$

$$
\begin{aligned}
&A^3_n\{\alpha_8(\nabla s)^2-\rho\alpha\} + 2\alpha_8(\nabla s.\nabla)A^3_{n-1} + \alpha_8\nabla^2 s\ A^3_{n-1}-\lambda h(\underset{\sim}{A}_{n-1}.\nabla s) \\
&+ \alpha_8\nabla^2 A^3_{n-2}-(\lambda+2\mu)A^3_{n-2}-\lambda h(\nabla.\underset{\sim}{A}_{n-2}) = 0 \ . \qquad (2.57)
\end{aligned}
$$

The above equations govern waves of the type (2.55) within the framework of the extensional theory.

Similarly substituting equation (2.55) into equations (2.3) and (2.4) with $\underset{\sim}{f}_2 = 0$, setting $\underset{\sim}{A}_{2n} = (\underset{\sim}{B}_n, B^3_n)$ we obtain for the bending theory the recurrence relations

$$
\begin{aligned}
&\underset{\sim}{B}_n\{(\nabla s)^2-\rho(\mu h)^{-1}\}+\frac{(3\lambda+2\mu)}{(\lambda+2\mu)}\nabla s(\underset{\sim}{B}_n.\nabla s) + 2(\nabla s.\nabla)\underset{\sim}{B}_{n-1} + \nabla^2 s\ \underset{\sim}{B}_{n-1} \\
&+ \frac{(3\lambda+2\mu)}{(\lambda+2\mu)}\{\nabla s(\nabla.\underset{\sim}{B}_{n-1})+ \nabla(\underset{\sim}{B}_{n-1}.\nabla s) + \nabla(\nabla.\underset{\sim}{B}_{n-2})\} \qquad (2.58) \\
&+ \nabla^2\underset{\sim}{B}_{n-2}-\alpha_3(\mu h\alpha)^{-1}\{B^3_{n-1}\nabla s + \underset{\sim}{B}_{n-2} + \nabla B^3_{n-2}\} = 0 \quad ,
\end{aligned}
$$

$$
\begin{aligned}
&B^3_n\{(\nabla s)^2-\rho\alpha_3^{-1}\} + 2(\nabla s.\nabla)B^3_{n-1} + \nabla^2 s\ B^3_{n-1} + \underset{\sim}{B}_{n-1}.\nabla s \\
&+ \nabla.\underset{\sim}{B}_{n-2} + \nabla^2 B^3_{n-2} = 0 \ . \qquad (2.59)
\end{aligned}
$$

In equations (2.56)-(2.59) we set the leading term $\underset{\sim}{A}_{\alpha o} = 0$, an assumption which is consistent with the case of first order waves. In addition, we set

$$S = G^{-1}\psi \; , \; \underset{\sim}{A}_{\alpha n} = (-1)^n [\underset{\sim\sim}{w}_{\alpha , n}] \; , \; n \geq 1 \quad , \tag{2.60}$$

in the recurrence relations (2.56)-(2.59). If we now put n = 1 in equations (2.56) and (2.57) and take the scalar product of equation (2.56) with $\underset{\sim}{\lambda}$ and $\underset{\sim}{\nu}$, we obtain the set of equations (2.26) and note that the magnitude $|\nabla S| = G^{-1}$. Thus it follows immediately that the classification of harmonic extensional waves corresponds directly to those of the extensional pulse propagation case. In addition, the equations (2.56) and (2.57) for $n \geq 1$, yield a set of equations which are precisely the transport-induction equations given in the previous section for the extensional pulse propagation problem. Entirely analogous remarks and results pertain to equations (2.58) and (2.59) and the corresponding bending wave classification and transport-induction equations given in section 2.2.

We thus see that there is a one to one correspondence between pulse solutions in the form (2.8) and steady state time harmonic solutions (2.55). For a given set of boundary conditions, solution of the transport-induction equations given in section 2.2, simultaneously solves each of these problems. The method of obtaining the transport-induction equations by using asymptotic series of the type (2.55) is called the Karal-Keller technique [10]. We note that the geometric acoustics solution corresponds to the leading term in equation (2.55) and hence for large ω, the amplitude of the harmonic solution decays as the geometrical acoustics solution. Moreover, the curves of constant phase correspond to the wave fronts in the pulse propagation problem, and we may regard this leading term as representing a decaying harmonic wave whose phase velocity is equal to the wave front velocity.

We shall now give a specific example of the aforementioned correspondence. Define the *unit pulse* solution $\underset{\sim}{w}_{\alpha}^{H}$ as the transient solution of equation (2.7) with $\underset{\sim}{f}_{\alpha} = 0$ satisfying the boundary condition

$$\dot{\underset{\sim}{w}}_{\alpha}^{H} = \dot{\underset{\sim}{w}}_{\alpha o} H(t) \quad , \tag{2.61}$$

where $\dot{\underset{\sim}{w}}_{\alpha o} = \dot{\underset{\sim}{w}}_{\alpha o}(\ell)$ is specified on an initial curve C_o in the plate and H(t) is the Heaviside function.[3] From equations (2.55) and (2.60) one sees that corresponding to $\underset{\sim}{w}_{\alpha}^{H}$ will be a steady state time harmonic solution $\underset{\sim}{w}_{\alpha}^{\omega}$ of equation (2.7) with $\underset{\sim}{f}_{\alpha} = 0$, satisfying the boundary condition

$$\dot{\underset{\sim}{w}}_{\alpha}^{\omega} = \dot{\underset{\sim}{w}}_{\alpha o} e^{-i\omega t} \quad , \tag{2.62}$$

on the initial curve C_o.

An alternate procedure for showing this correspondence between $\underset{\sim}{w}_{\alpha}^{H}$ and $\underset{\sim}{w}_{\alpha}^{\omega}$ may be produced by following an analysis similar to that used in [5]. The transient solution to equation (2.7) satisfying an arbitrary time dependent boundary condition

$$\dot{\underset{\sim}{w}}_{\alpha} = \dot{\underset{\sim}{w}}_{\alpha o} f(t) \quad , \tag{2.63}$$

on C_o, may be given in the form of a Duhamel integral [9] as

---

[3] The Heaviside function is defined by $H(t) = 0$, $t < 0$, and $H(t) = 1$, $t > 0$. It is related to the Dirac delta function by $\Delta(t) = \dot{H}(t)$, where the differentiation is in the generalised sense [8].

$$\underset{\sim}{w}_\alpha = \frac{\partial}{\partial t}\int_0^t \underset{\sim}{w}_\alpha^H(t-\tau)f(\tau)dt \quad . \tag{2.64}$$

Applying equation (2.63) to the choice $f(t) = H(t)e^{-i\omega t}$, after repeated integration by parts and letting $t \to \infty$, we obtain a steady state solution in the form of the series (2.55) with $\underset{\sim}{A}_{\alpha o} = 0$ and $\underset{\sim}{A}_{\alpha n} = (-1)\ [\underset{\sim\sim}{w}^H_{\alpha,n}]$, for $n \geq 1$.[4] Equation (2.64) may be written in the equivalent form

$$\underset{\sim}{w}_\alpha = \int_0^t \underset{\sim}{w}_\alpha^\Delta(t-\tau)f(\tau)dt \quad . \tag{2.65}$$

where

$$\underset{\sim}{w}_\alpha^\Delta = \dot{\underset{\sim}{w}}_\alpha^H \quad . \tag{2.66}$$

We observe that $\underset{\sim}{w}_\alpha^\Delta$ is a Green's function for the problem at hand. It corresponds to what may be termed the *unit impulse* solution of equation (2.7), arising due to the boundary condition

$$\dot{\underset{\sim}{w}}_\alpha^\Delta = \dot{\underset{\sim}{w}}_{\alpha o}\Delta(t) \quad , \tag{2.67}$$

on C_o.[5]

Once a unit pulse solution $\underset{\sim}{w}_\alpha^H$ has been found for any boundary we could use it to find solutions corresponding to arbitrary time dependence on the boundary. On the other hand if this time dependence is Fourier analyzed to obtain its frequency spectrum, then we can use the time harmonic solution $\underset{\sim}{w}_\alpha^\omega$ to obtain solutions by Fourier *synthesis*.

---

[4] In actual fact we obtain up to three series of this type for each $\alpha = 1,2$, depending upon how many of the wave surfaces $\phi(x,y,t) = 0$ make contributions on being crossed in the integration process.

[5] We observe that the solution $\underset{\sim}{w}_\alpha^\Delta$ corresponds to a zeroth order wave, which is inadmissible on physical grounds. However, if we think of this solution as giving velocity (or strain) rather than displacement it raises no conceptual problem.

2.4 Uncoupled Wave Motions

In general, for each of the classes of extensional and bending waves, coupling will occur between the various wave types. As seen in [11] this is true even in the case of plane waves, where coupling occurs between the longitudinal and squeeze gradient waves within the framework of the extensional theory and between the bending and kink waves within the framework of the bending theory. The shear and twisting waves were uncoupled and might be referred to as *pure* waves. Our objective here is to see if it is possible to expand the category of pure plane waves. This in fact can be done by introducing suitable constrained motions, for which the constraints are produced by application of appropriate body forces $\underset{\sim}{f}_\alpha$.

(i) *Pure Tilting and Twisting Waves*

In equations (2.3), (2.4) we assume $\underset{\sim}{w}_2 = \underset{\sim}{w}_2(x,t)$, $\underset{\sim}{\delta} = \delta^1 \underset{\sim}{i} + \delta^2 \underset{\sim}{j}$, $u^3 = 0$, $\underset{\sim}{L} = 0$, where $\underset{\sim}{i}, \underset{\sim}{j}$ are unit vectors along the rectangular cartesian coordinate axes x,y. We obtain,

$$\frac{\partial^2 \delta^1}{\partial t^2} - G_B^2 \frac{\partial^2 \delta^1}{\partial x^2} + \frac{G_K^2}{\alpha} \delta^1 = 0 \quad , \quad F^3 = -\frac{\alpha_3}{\rho} \frac{\partial \delta^1}{\partial x} \quad , \tag{2.68}$$

$$\frac{\partial^2 \delta^2}{\partial t^2} - G_T^2 \frac{\partial^2 \delta^2}{\partial x^2} + \frac{G_K^2}{\alpha} \delta^2 = 0 \quad . \tag{2.69}$$

Equation $(2.68)_1$ defining a pure tilting[6] wave corresponds to a tilting of the plate cross-section and requires a

[6] Logically we should call this wave a pure bending wave, but since this terminology usually has another meaning and since the terminology tilting is descriptive, we introduce it here.

constraining body force given by equation $(2.68)_2$. This constraint can be maintained by sandwiching the plate between two rigid layers. Equation (2.69) defines a pure twisting wave and its existence requires no constraint.

(ii) *Pure Shear and Squeeze Gradient Waves*

In equations (2.1) and (2.2) we assume $\underset{\sim}{w}_1 = \underset{\sim}{w}_1(x,t)$, $\underset{\sim}{u} = u^1\underset{\sim}{i} + u^2\underset{\sim}{j}$, $u^1 = 0$, $L^3 = 0$, $\underset{\sim}{F} = F^1\underset{\sim}{i}$ and find that these conditions are satisfied provided

$$\frac{\partial^2\delta^3}{\partial t^2} - G_S^2\,\frac{\partial^2\delta^3}{\partial x^2} + \frac{G_L^2}{\alpha}\,\delta^3 = 0 \;,\; F^1 = -\,\frac{\lambda h}{\rho}\,\frac{\partial\delta^3}{\partial x} \;, \tag{2.70}$$

$$\frac{\partial^2 u^2}{\partial t^2} - G_T^2\,\frac{\partial^2 u^2}{\partial x^2} = 0 \;. \tag{2.71}$$

Equation (2.70) defines a pure squeeze gradient wave and requires that the plate midsurface be made inextensible. Equation (2.71) governs the propagation of pure shear waves and their existence requires no constraint.

(iii) *Pure Kink Waves*

In equation (2.3) and (2.4) we now assume $\underset{\sim}{w}_2 = \underset{\sim}{w}_2(x,t)$, $F^3 = -\,\frac{K}{\rho}\,u^3$, $K \geq 0$, $\underset{\sim}{\delta} = 0$, $\underset{\sim}{L} = L^1\underset{\sim}{i}$ and we obtain the governing equation of a plane kink wave as

$$\frac{\partial^2 u^3}{\partial t^2} - G_K^2\,\frac{\partial^2 u^3}{\partial x^2} + K\,G_K^2 u^3 = 0 \;,\; L^1 = G_K^2\,\frac{\partial u^3}{\partial x} \;. \tag{2.72}$$

In order that this wave propagates, a constraining couple L^1 must be applied in order to assure that normals to the plane of the plate are constrained to remain normal. In the case $K \neq 0$, the problem corresponds to a plate on an elastic foundation with modulus K.

We note that each of the waves defined by equations (2.68)-(2.70) and (2.72) satisfy the same differential equation and some form of constraining equation and hence it is only necessary to deal with one of these in order to solve them all. The governing transport equation [7] may be obtained by making the appropriate substitutions in the appropriate general forms of these in section 2.2, or by directly seeking a solution to equation $(2.68)_1$ in the form (2.55). An example will be considered in the next section.

The pure shear and twisting plane waves defined by equations (2.71) and (2.69) may be generalized. By examining the induction equations (2.34), (2.35) and (2.46), (2.47), which correspond to these two types of waves, we see that no coupling will exist provided the wave discontinuities are constant along the wave fronts. From the form of the transport equations we see that this will be true only if the wave curves are of constant curvature, i.e. circular and if the discontinuities are constant on the initial wave curve. Hence we can have pure shear and twisting waves with circular wave fronts.

---

[7] Since there is no coupling, the induction equations make no contribution to the analysis. They are replaced by the approoriate constraint equations. For the case $K \neq 0$, the transport equation (2.49) for the kink wave does not apply, as it was derived on the basis of C^∞ body forces.

2.5 Examples

(i) *Torsional Shear Waves*

We consider the problem of an unbounded plate having a circular cavity of radius a_o and subjected to a steady state time harmonic uniform shear stress. For this problem the curves of constant phase will be concentric circles and it is natural to employ plane polar coordinates (r,θ) to formulate the problem. If we assume

$$\underset{\sim}{u} = u(r)\underset{\sim}{\lambda} \ , \ \delta^3 = 0 \ , \ \underset{\sim 1}{f} = 0 \ , \ L^3 = 0 \ , \qquad (2.73)$$

then the governing equations (2.1) and (2.2) reduce to

$$\frac{\partial^2 u}{\partial r^2} + \frac{1}{r}\frac{\partial u}{\partial r} - \frac{u}{r^2} = \frac{1}{G_T^2}\frac{\partial^2 u}{\partial t^2} \ , \qquad (2.74)$$

where u denotes the circumferential component of displacement. The appropriate boundary condition is

$$\tau_{r\theta} = \mu\left(\frac{\partial u}{\partial r} - \frac{u}{r}\right) = \tau_o e^{-i\omega t} \text{ at } r = a_o \ , \qquad (2.75)$$

where τ_o is a constant. From equations (2.33), $(2.60)_2$, (2.53) and (2.54) we obtain the solution to the appropriate transport equation as

$$A_n = A_n(a_o)\frac{a_o^{\frac{1}{2}}}{r^{\frac{1}{2}}} - \frac{G_T}{2r^{\frac{1}{2}}}\int_{a_o}^{r}(\tau^{\frac{1}{2}})\left(\frac{d^2A_{n-1}}{dr^2} + \frac{1}{r}\frac{dA_{n-1}}{dr} - \frac{A_{n-1}}{r^2}\right)(\tau)d\tau. \quad (2.76)$$

From equations (2.75) and (2.76) we obtain

$$A_1 = \frac{\tau_o G_T}{\mu}\left(\frac{a_o}{r}\right)^{\frac{1}{2}}, \; A_2 = \frac{3\tau_o G_T^2}{8\mu a_o}\left\{5\left(\frac{a_o}{r}\right)^{\frac{1}{2}} - \left(\frac{a_o}{r}\right)^{\frac{3}{2}}\right\},$$

$$A_3 = \frac{15\tau_o G_T^3}{128\mu a_o^3}\left\{23\left(\frac{a_o}{r}\right)^{\frac{1}{2}} - 6\left(\frac{a_o}{r}\right)^{\frac{3}{2}} - \left(\frac{a_o}{r}\right)^{\frac{5}{2}}\right\}, \text{ etc.} \tag{2.77}$$

Moreover since $|\nabla S| = G_T^{-1}$, we also find

$$S = (r-a_o)/G_T \quad . \tag{2.78}$$

The solution to the problem is given by equation (2.55) on setting $\underset{\sim}{w}_1 = u\underset{\sim}{\lambda}$ and $\underset{\sim}{A}_{1n} = A_n\underset{\sim}{\lambda}$ and utilising equations (2.77) and (2.78).

The solution to the corresponding unit pulse problem is given by

$$u^H = \sum_{n=1}^{\infty} (-1)^n \frac{A_n}{n!} \langle t-(r-a_o)/G_T\rangle^n \quad . \tag{2.79}$$

The resulting shear stress may now be calculated from equations $(2.75)_1$ and (2.79). This problem has been solved in closed form by Goodier and Jahsman [12], using Laplace transform techniques. Achenbach in [4] dealt with the solution via discontinuity analysis, proceeding in a slightly different but equivalent fashion to that employed here. To illustrate the efficiency of the procedure we compute the shear stress using the three coefficients given in equation (2.77). The results are plotted in Figure 2 where they are compared with the exact analysis of [12]. The first term alone in the series gives the wave front solution and hence the perfect agreement in the peak values. By using additional terms in the series (2.79) we could improve the agreement elsewhere. Similar results for the velocity $\dot{u}^H$ showed analogous comparison with those in [12].

(ii) *Pure Tilting Waves*

As an illustration of the class of constrained waves discussed earlier, we deal with pure tilting waves as governed by equation $(2.68)_1$ and subject to the boundary condition

$$\frac{\partial\delta}{\partial x} = e^{-i\omega t}, \text{ at } x = 0 \quad , \tag{2.80}$$

where for convenience we have set $\delta^1 = \delta$. From equations (2.41), $(2.60)_2$ and conditions leading to equation (2.68) we find the required transport equation to be

$$\frac{dB_n}{dx} = \frac{b^2}{2G_B} B_{n-1} - \frac{G_B}{2}\frac{d^2B_{n-1}}{dx^2} \quad , \; b^2 = G_K^2\alpha^{-1} \quad , \; n \geq 1 \quad , \tag{2.81}$$

where $\underset{\sim}{A}_{2n} = B_n \underset{\sim}{\nu}$. From $|\nabla S| = G_B^{-1}$ and equation (2.80) we find

$$S = \frac{x}{G_B} \quad , \tag{2.82}$$

while equations (2.81) subject to (2.80) have the solution

$$B_{n+1} = -G_B n! \sum_{m=n}^{n} \left(\frac{b}{2}\right)^{2m} \frac{1}{(m!)^2} \sum_{k=\bar{n}}^{m} (-1)^{2m-k+n} \binom{m}{k}\binom{2k}{n}\left(\frac{x}{G_B}\right)^{2m-n} , \tag{2.83}$$

where $\bar{n} = \frac{n}{2}$ for even n and $\frac{n+1}{2}$ for odd n, $n \geq 0$ and $\binom{m}{k} = \frac{m!}{(m-k)!k!}$. Substituting equation (2.82) and (2.83) into equation (2.55) with $\underset{\sim}{w}_2 = \delta\underset{\sim}{\nu}$ and $\underset{\sim}{A}_{2n} = B_n\underset{\sim}{\nu}$ gives the solution to the posed time harmonic problem. The constraining body force may be calculated using equation $(2.68)_2$.

The solution to the corresponding unit pulse problem i.e. one for which

$$\frac{\partial \delta}{\partial x} = H(t) \quad , \text{ at } x = 0 \quad , \tag{2.84}$$

is given by

$$\delta^H = \sum_{n=1}^{\infty} (-1)^n \frac{B_n}{n!} \langle t-\frac{x}{G_B}\rangle^n \quad . \tag{2.85}$$

This solution can be used to obtain the Green's function δ^{Δ} by application of equation (2.66), i.e. $\delta^{\Delta} = \dot{\delta}^H$.

Closed forms for the time-harmonic solution δ^{ω} and unit impulse solution δ^{Δ} may be obtained from equation (2.68), by the methods of separation of variables and Laplace transforms, respectively. These are given in [13] and are

$$\delta^{\omega} = -\frac{G_B \, e^{i(kx-\omega t)}}{(i\omega)\,(1-\frac{b^2}{\omega^2})^{\frac{1}{2}}} \quad , \; k^2 = \frac{\omega^2}{G_B^2}(1-\frac{b^2}{\omega^2}) \quad , \tag{2.86}$$

$$\delta^{\Delta} = G_B \, J_o \, (b^2t^2 - \frac{x^2b^2}{G_B^2})^{\frac{1}{2}} \quad , \; t > \frac{x}{G_B} \quad , \tag{2.87}$$

where J_o is the Bessel function of order zero. When equation (2.86) is expanded in inverse powers of $(i\omega)$, we obtain term by term agreement with our time harmonic solution as given by equations (2.55), (2.82) and (2.83). Moreover, when the Bessel's function in equation (2.87) is expanded as a Taylor series about $t = \frac{x}{G_B}$, we obtain precisely the series for δ^{Δ} obtained by differentiating equation (2.85) .

CHAPTER III

AXI-SYMMETRIC TRANSIENTS IN SHELLS OF REVOLUTION

3.1 Equations of Motion

We now consider the propagation of axi-symmetric transients in linear, isotropic and homogeneous shells of revolution with straight line generators. Thus the solutions to be presented in this chapter are applicable to conical and cylindrical shells and to circular plates. We utilise Naghdi's equations [1] which are based on the Cosserat theory and which include the effects of transverse shear, transverse normal stress and strain and rotatory inertia. If the meridional and normal displacements of the shell midsurface, the rotation of the normal to this surface about the tangential direction and the transverse normal strain are denoted by u, w, ψ_s, ψ_z respectively, the displacement equations of motion can be written as

$$\frac{\partial^2 u}{\partial s^2} - \frac{1}{G_L^2}\frac{\partial^2 u}{\partial t^2} = \sum_{i=1}^{8} a_{io} V_{io} \quad , \tag{3.1}$$

$$\frac{\partial^2 \psi_s}{\partial s^2} - \frac{1}{G_B^2}\frac{\partial^2 \psi_s}{\partial t^2} = \sum_{i=1}^{8} b_{io} V_{io} \quad , \tag{3.2}$$

$$\frac{\partial^2 w}{\partial s^2} - \frac{1}{G_K^2}\frac{\partial^2 w}{\partial t^2} = \sum_{i=1}^{8} c_{io} V_{io} \quad , \tag{3.3}$$

$$\frac{\partial^2 \psi_z}{\partial s^2} - \frac{1}{G_S^2}\frac{\partial^2 \psi_z}{\partial t^2} = \sum_{i=1}^{8} d_{io} V_{io} \quad . \tag{3.4}$$

In the above equations s is the meridional co-ordinate and the wavefront speeds are as given below:

$$G_L^2 = C(1-\nu)/(1-2\nu)\rho,\ G_B^2 = C/\rho,\ G_K^2 = \alpha_3/\rho,\ G_S^2 = \alpha_8/\rho\alpha \quad , \qquad (3.5)$$

where ν is the Poisson's ratio, ρ the density, $\alpha = h^2/12$, h being the thickness, $C = E/(1-\nu^2)$, E being the Young's modulus and the material constants α_3, α_8 are taken as having the approximate values $5E/12(1+\nu)$ and $7E\alpha/20(1+\nu)$ respectively. Moreover the quantities V_{io} are given by

$$\begin{aligned} V_{10} &= \frac{\partial u}{\partial s},\ V_{20} = u,\ V_{30} = \frac{\partial \psi_s}{\partial s},\ V_{40} = \psi_s, \\ V_{50} &= \frac{\partial w}{\partial s},\ V_{60} = w,\ V_{70} = \frac{\partial \psi_z}{\partial s},\ V_{80} = \psi_z, \end{aligned} \qquad (3.6)$$

and the coefficients a_{io}, b_{io}, c_{io}, d_{io} which contain the material and geometric properties of the shell are given in the Appendix I.

The equations of motion corresponding to the uniaxial theory [16] and the modified membrane and bending theories of Mortimer et al [18], [19] can be obtained from equations (3.1)-(3.4) by assigning appropriate values to the coefficients a_{io}, b_{io}, c_{io}, and d_{io}. Thus the solutions that will be presented could also be utilised to obtain those corresponding to the above mentioned theories.

Due to the presence of lower order derivatives, equations (3.1)-(3.4) are dispersive [2], causing transient waves to be distorted and the phase velocities of time harmonic waves to be frequency dependent. However, these equations do not contain mixed spatial and temporal derivatives and are hyperbolic, ensuring finite wavefront speeds for transients and bounded phase velocities for time harmonic waves [3]. For this reason these equations become very suitable for solution by the method of discontinuity analysis or by the method of characteristics [18], [19].

3.2 Method of Solution

The method of discontinuity analysis is well known and is described in detail by Achenbach [4] and by Kline and Kay [5]. According to this method a wave is considered as a carrier of discontinuities in the field variable and/or its derivatives. These discontinuities satisfy certain conditions at the wavefront from which it is possible to obtain a set of recursive relations known as the transport-induction equations. These equations govern the propagation of the discontinuities of all order at the wavefront, and determine them if the boundary condition is known. The transient solution due to time dependent loads acting at the boundary of a structure can then be determined in the form of a Taylor series expansion behind the wavefront. This is the method suggested by Achenbach [4], and we call it the direct method.

The time dependent loads that we consider, are those that act for a finite time and are specified in the form of strain, velocity or acceleration boundary conditions. For these cases the direct method if applicable, will be tedious and it is preferable to utilise the Green's function concept. We define the unit pulse solution as the transient solution corresponding to the boundary condition involving the Heaviside step function. The unit pulse solution can easily be determined by the direct method and then its time derivative gives us the Green's function for the problem at hand [9]. The Duhamel integral together with the Green's function will then give us, at least numerically, the required solution to any transient problem.

The solution to the corresponding time harmonic problem can be determined by the Karal-Keller technique [10]. According to this we formally assume asymptotic time harmonic series solutions to the equations. The coefficients of these series are found to satisfy a set of differential recurrence relations which are exactly the transport-induction equations discussed above. There is found to exist a one to one relationship between the unit pulse problem and the corresponding time-harmonic problem. In practice for a given set of equations of motion, it is much simpler to generate the transport-induction equations by the Karal-Keller technique than by the method of discontinuity analysis.

To this end, we assume time-harmonic solutions to equations (3.1)-(3.4) in the form

$$
\begin{aligned}
u &= e^{i\omega(S-t)} \sum_{n=1}^{\infty} \frac{A_n}{(i\omega)^n}, \quad \psi_s = e^{i\omega(S-t)} \sum_{n=1}^{\infty} \frac{B_n}{(i\omega)^n} \\
w &= e^{i\omega(S-t)} \sum_{n=1}^{\infty} \frac{C_n}{(i\omega)^n}, \quad \psi_z = e^{i\omega(S-t)} \sum_{n=1}^{\infty} \frac{D_n}{(i\omega)^n},
\end{aligned}
\tag{3.7}
$$

where S is the phase function, ω the circular frequency and the amplitude functions of the time harmonic series are given by

$$A_n=(-1)^n[\underset{\sim}{u}^H_{,n}],B_n=(-1)^n[\underset{\sim}{\psi}^H_{s,n}],C_n=(-1)^n[\underset{\sim}{w}^H_{,n}],D_n=(-1)^n[\underset{\sim}{\psi}^H_{z,n}]. \quad (3.8)$$

In the above equations $\underset{\sim}{[}\ \underset{\sim}{]}$ indicates the discontinuity or jump of the argument across the wavefront , the comma followed by n denotes n^{th} order time derivative and the superscript H denotes the unit pulse solution. On substituting equations (3.7) into equations (3.1)-(3.4) and formally requiring that the coefficients of powers of $(i\omega)$ separately vanish, we obtain the recurrence relations for $n \geq 1$ as

$$A_n(1-G^2/G_L^2) + 2G\frac{dA_{n-1}}{ds} - Ga_{10}A_{n-1} = G^2\bar{T}^A_{n-2}\ , \quad (3.9)$$

$$B_n(1-G^2/G_B^2) + 2G\frac{dB_{n-1}}{ds} - Gb_{30}B_{n-1} = G^2\bar{T}^B_{n-2}\ , \quad (3.10)$$

$$C_n(1-G^2/G_K^2) + 2G\frac{dC_{n-1}}{ds} - Gc_{50}C_{n-1} = G^2\bar{T}^C_{n-2}\ , \quad (3.11)$$

$$D_n(1-G^2/G_S^2) + 2G\frac{dD_{n-1}}{ds} - Gd_{70}D_{n-1} = G^2\bar{T}^D_{n-2}\ . \quad (3.12)$$

In equations (3.9)-(3.12), G is the wavefront speed, related to S in the form

$$\frac{dS}{ds} = \frac{1}{G}\ , \quad (3.13)$$

and

$$\bar{T}^A_{n-2} = -\frac{d^2A_{n-2}}{ds^2} + a_{10}\frac{dA_{n-2}}{ds} + a_{20}A_{n-2} + a_{30}\left(\frac{B_{n-1}}{G}+\frac{dB_{n-2}}{ds}\right) + a_{40}B_{n-2}$$

$$+ a_{50}\left(\frac{C_{n-1}}{G}+\frac{dC_{n-2}}{ds}\right) + a_{60}C_{n-2} + a_{70}\left(\frac{D_{n-1}}{G}+\frac{dD_{n-2}}{ds}\right) + a_{80}D_{n-2}\ , \quad (3.14)$$

$$\bar{T}^B_{n-2} = -\frac{d^2B_{n-2}}{ds^2} + b_{10}\left(\frac{A_{n-1}}{G} + \frac{dA_{n-2}}{ds}\right) + b_{20}A_{n-2} + b_{30}\frac{dB_{n-2}}{ds} + b_{40}B_{n-2}$$

$$+ b_{50}\left(\frac{C_{n-1}}{G} + \frac{dC_{n-2}}{ds}\right) + b_{60}C_{n-2} + b_{70}\left(\frac{D_{n-1}}{G} + \frac{dD_{n-2}}{ds}\right) + b_{80}D_{n-2}\,, \tag{3.15}$$

$$\bar{T}^C_{n-2} = -\frac{d^2C_{n-2}}{ds^2} + c_{10}\left(\frac{A_{n-1}}{G} + \frac{dA_{n-2}}{ds}\right) + c_{20}A_{n-2} + c_{30}\left(\frac{B_{n-1}}{G} + \frac{dB_{n-2}}{ds}\right)$$

$$+ c_{40}B_{n-2} + c_{50}\frac{dC_{n-2}}{ds} + c_{60}C_{n-2} + c_{70}\left(\frac{D_{n-1}}{G} + \frac{dD_{n-2}}{ds}\right) + c_{80}D_{n-2}\,, \tag{3.16}$$

$$\bar{T}^D_{n-2} = -\frac{d^2C_{n-2}}{ds^2} + d_{10}\left(\frac{A_{n-1}}{G} + \frac{dA_{n-2}}{ds}\right) + d_{20}A_{n-2} + d_{30}\left(\frac{B_{n-1}}{G} + \frac{dB_{n-2}}{ds}\right)$$

$$+ d_{40}B_{n-2} + d_{50}\left(\frac{C_{n-1}}{G} + \frac{dC_{n-2}}{ds}\right) + d_{60}C_{n-2} + d_{70}\frac{dD_{n-2}}{ds} \tag{3.17}$$

$$+ d_{80}D_{n-2}\,.$$

The lowest order derivative of the field variable (u, ψ_s, w, ψ_z) having a discontinuity defines the order of the wave. A first order wave is called a shock or strain wave and will constitute the subject matter dealt with herein. The results for higher order waves will be completely analagous to those of first order waves. Considering first order waves and setting n=1 in equations (3.9)-(3.12) we obtain,

$$(G^2 - G_L^2)A_1 = 0, \quad (G^2 - G_B^2)B_1 = 0, \quad (G^2 - G_K^2)C_1 = 0, \quad (G^2 - G_S^2)D_1 = 0\,. \tag{3.18}$$

From the above set of equations we can obtain the classification [14], speeds and propagation conditions for axi-symmetric first order waves. Moreover substituting the appropriate speed G in turn, into equations (3.9)-(3.12) with $n \geq 2$, we obtain the transport induction equations for each wave type. The transport equations will be first order ordinary differential equations and can readily be integrated. We present below the results for each case.

(i) *Longitudinal Waves*

$$G = G_L \;,\; A_1 \neq 0 \;,\; B_1 = 0 \;,\; C_1 = 0 \;,\; D_1 = 0 \quad . \tag{3.19}$$

$$A_n(s) = A_n(s_o)\left(\frac{s_o}{s}\right)^{\frac{1}{2}} + \frac{G}{2}\int_{s_o}^{s}\left(\frac{\tau}{s}\right)^{\frac{1}{2}} \bar{T}^A_{n-1}(\tau)\,d\tau \quad . \tag{3.20}$$

$$B_n = H^B_n \;,\; C_n = H^C_n \;,\; D_n = H^D_n \quad . \tag{3.21}$$

(ii) *Bending Waves*

$$G = G_B \;,\; B_1 \neq 0 \;,\; A_1 = 0 \;,\; C_1 = 0 \;,\; D_1 = 0 \quad . \tag{3.22}$$

$$B_n(s) = B_n(s_o)\left(\frac{s_o}{s}\right)^{\frac{1}{2}} + \frac{G}{2}\int_{s_o}^{s}\left(\frac{\tau}{s}\right)^{\frac{1}{2}} \bar{T}^B_{n-1}(\tau)\,d\tau \quad . \tag{3.23}$$

$$A_n = H^A_n \;,\; C_n = H^C_n \;,\; D_n = H^D_n \,. \tag{3.24}$$

(iii) *Kink Waves*

$$G = G_K \;,\; C_1 \neq 0 \;,\; A_1 = 0 \;,\; B_1 = 0 \;,\; D_1 = 0 \quad . \tag{3.25}$$

$$C_n(s) = C_n(s_o)\left(\frac{s_o}{s}\right)^{\frac{1}{2}} + \frac{G}{2}\int_{s_o}^{s}\left(\frac{\tau}{s}\right)^{\frac{1}{2}} \bar{T}^C_{n-1}(\tau)\,d\tau \quad . \tag{3.26}$$

$$A_n = H^A_n \;,\; B_n = H^B_n \;,\; D_n = H^D_n \,. \tag{3.27}$$

(iv) *Squeeze-Gradient Waves*

$$G = G_S \;,\; D_1 \neq 0 \;,\; A_1 = 0 \;,\; B_1 = 0 \;,\; C_1 = 0 \quad . \tag{3.28}$$

$$D_n(s) = D_n(s_o)\left(\frac{s_o}{s}\right)^{\frac{1}{2}} + \frac{G}{2}\int_{s_o}^{s}\left(\frac{\tau}{s}\right)^{\frac{1}{2}} \bar{T}^D_{n-1}(\tau)\,d\tau \quad . \tag{3.29}$$

$$A_n = H^A_n \; , \; B_n = H^B_n \; , \; C_n = H^C_n \quad . \tag{3.30}$$

In the above sets of equations H^A_n, H^B_n, H^C_n and H^D_n are functions of the wave speed G and are given by

$$H^A_n = \frac{G\ G^2_L}{G^2_L - G^2}\left\{ -\ 2\frac{dA_{n-1}}{ds} + a_{10}\, A_{n-1} + G\bar{T}^A_{n-2} \right\} , \tag{3.31}$$

$$H^B_n = \frac{G\ G^2_B}{G^2_B - G^2}\left\{ -\ 2\frac{dB_{n-1}}{ds} + b_{30}\, B_{n-1} + G\bar{T}^B_{n-2} \right\} , \tag{3.32}$$

$$H^C_n = \frac{G\ G^2_K}{G^2_K - G^2}\left\{ -\ 2\frac{dC_{n-1}}{ds} + c_{50}\, C_{n-1} + G\bar{T}^C_{n-2} \right\} , \tag{3.33}$$

$$H^D_n = \frac{G\ G^2_S}{G^2_S - G^2}\left\{ -\ 2\frac{dD_{n-1}}{ds} + d_{70}\, D_{n-1} + G\bar{T}^D_{n-2} \right\} , \tag{3.34}$$

For each wave type G denotes the eigenvalue corresponding to the eigenvector (A_1, B_1, C_1, D_1). The equation with the integral is the solution to the transport equation and the set of three following it are the induction equations. The boundary value of s is denoted by s_o. Moreover for cylindrical shells the quantities $(s_o/s)^{\frac{1}{2}}$ and $(\tau/s)^{\frac{1}{2}}$ appearing in the transport equations are to be replaced by unity. We utilise the boundary conditions, equation (3.8) and the appropriate transport-induction equations to determine the required discontinuities. The corresponding unit pulse solution U^H is then given by the Taylor series

$$U^H = \sum_{n=1}^{\infty} [U^H_{,n}]\langle t-S\rangle^n/n! \quad , \tag{3.35}$$

with

$$S = S(s_o) + (s-s_o)/G \quad , \tag{3.36}$$

where U stands for any one of the field variables u, ψ_s, w or ψ_z, and $\langle\ \rangle = 0$, if the argument is negative. The required transient solution is then given by [9]

$$U = \int_0^t \frac{\partial U^H(t-\tau)}{\partial t} f(\tau)\,d\tau \quad , \tag{3.37}$$

where $f(\tau)$ is the time dependence of the boundary data. The results for second order or acceleration waves could be obtained in an analagous manner by starting with n=2, in equations (3.7)-(3.12).

In section 3.4, we will use the results presented above to solve some numerical problems, after discussing a numerical scheme for the solution, in the next section.

3.3 Superposition Technique

Our experience in the numerical evaluation of the series solutions given by equations (3.35) and (3.37) indicates that their convergence is usually slow. This is especially so at large values of T = (t-S), the time elapsed after the wavefront. The problem is similar to that in the evaluation of exp(-T) for large values of T, using its Taylor series expansion.

Although we expect an improvement if the number of terms in equations (3.35) or (3.37) is increased, in practice the task becomes very tedious. Moreover beyond a critical value $T = T_o$, the numerical convergence of the series is lost no matter how many terms are computed [15]. Mainardi and Turchetti [15] have introduced Padē approximants to accelerate the convergence of series solutions of the types in equations (3.35) or (3.37) for the case of viscoelastic waves. We have devised a numerical superposition technique that assures convergence in all cases. Furthermore, we have verified that the results obtained by incorporating this technique agree with those of Mainardi and Turchetti.

For a boundary load of the step type having a magnitude of unity and a duration t_o, acting on a structure, we know that on physical grounds the response at any location must decay to zero after some time [20]. By choosing a small enough value for t_o, say t_o^*, it is possible in most cases to obtain a response that decays to zero by using a few terms in the series (3.35) together with the Duhamel integral, equation (3.37). To such a response we give the name "test solution". Thus the test solution is assumed to be zero after a definite period of time. A typical test solution for the strain response due to a first order (strain or velocity) boundary condition is shown in Figure 3a. The given boundary load is then subdivided into step loads of duration t_o^* as shown in Figure 3b, where the magnitude of a step load is equal to the mean value of the boundary load during the appropriate time. We then solve the equivalent problem by considering the superposition of the responses due to each step load originating from the boundary at the appropriate time.

In the examples considered in the next section the superposition technique is applied. The solutions obtained without and with the incorporation of this technique will be denoted by "series solutions" and "modified solutions" respectively.

We used the superposition technique to solve the problem considered in example 1 of section 2.5 in the previous chapter. The series and modified solutions are shown in Figure 2. We observe the good agreement between the modified solution and the solution obtained by Goodier using Laplace transforms.

3.4 Numerical Examples and Discussion

3.4.1 Example 1: - Longitudinal Impact of a Conical Shell

We consider the transient response of a truncated conical shell which is impacted at its smaller end. Utilising the uniaxial theory and Laplace transforms, this problem was solved by Kenner et al [16]. Cohen and Berkel [21] obtained the wavefront solution for the same problem, using the method of discontinuity analysis. The relevant boundary condition is

$$\frac{\partial u}{\partial s}(s_o,t) = \begin{cases} E_o \sin^2 \pi t/t_o , & 0 \le t \le t_o \\ 0 , & t \ge t_o \end{cases} \tag{3.38}$$

where E_o is a constant.

To obtain the solution corresponding to the uniaxial theory, we consider the transport equation (3.20) for the longitudinal wave and set the coefficients a_{io}, i = 1-8, zero. The appropriate boundary condition for the unit pulse solution, together with equation $(3.7)_1$ yields

$$A_n(s_o) = 1; \; A_n(s_o) = -G_L \left.\frac{dA_{n-1}}{ds}\right|_{s=s_o}, \; n \geq 2; \; S(s_o) = 0 \; . \tag{3.39}$$

From equations (3.20) and (3.39) we obtain,

$$\begin{aligned} A_1 &= E_o G_L (s_o/s)^{\frac{1}{2}} \; , \; A_2 = E_o G_L^2 \{3(s_o/s)^{\frac{1}{2}} + (s_o/s)^{\frac{3}{2}}\}/8s_o \; , \\ A_3 &= 3E_o G_L^2 \{11(s_o/s)^{\frac{1}{2}} + 2(s_o/s)^{\frac{3}{2}} + 3(s_o/s)^{\frac{5}{2}}\}/128 s_o^2 \; , \text{ etc.} \end{aligned} \tag{3.40}$$

For this problem based on the uniaxial theory, $\nu = 0$ giving us $G_L^2 = E/\rho$. Using equations $(3.8)_1$, (3.37), (3.38) and (3.40) we obtain the transient solution as

$$u = \sum_{n=1} \frac{(-1)^n A_n}{(n-1)!} \int_o^t \langle t-\tau-S \rangle^{n-1} \sin^2(\pi\tau/t_o)\, d\tau \quad . \tag{3.41}$$

For s = 5.6cm the strains $\frac{\partial u}{\partial s}$ obtained from equation (3.41), using six terms for the cases t_o = 11μ secs, t_o = 22μ secs are shown in Figure 4a and that using nine terms for the case t_o = 50μ secs is shown in Figure 4b. These are the series solutions. The corresponding strains obtained by Kenner et al are also shown in these figures.

The boundary condition for the test solution is

$$\frac{\partial u}{\partial s}(s_o, t) = \begin{cases} 1, & 0 \le t \le t_o^* \\ 0, & t > t_o^* \end{cases} . \qquad (3.42)$$

Using $t_o^* = 0.5$ μ secs and four terms in equation (3.37) we constructed the test solution. The modified solution for each case is obtained by using the superposition technique together with equation (3.38). The results so obtained are also shown in Figures 4a and 4b.

We observe that for the cases $t_o = 11$ μ secs and $t_o = 22$ μ secs, the series solutions agree well with Kenner's solutions. Moreover the peak values for these cases match exactly. However for the case $t_o = 50$ μ secs, the series solution begins to diverge beyond $T = 30$ μ secs. No improvement was observed by doubling the number of terms in the series solution. The modified solutions not only showed better agreement with the results of Kenner for the cases $t_o = 11$ and $t_o = 22$ μ secs, but also provided us with comparable results for the case $t_o = 50$ μ secs. Similar solutions at other locations showed analogous comparisons with those of Kenner. By decreasing the value of t_o^*, we can expect an almost perfect agreement.

3.4.2 Example 2: - Cylindrical Tank Subjected to Vertical Ground Velocity Pulses

We consider the reinforced concrete cylindrical tank discussed by Billington [22] having a mean radius $a = 8.23$m, thickness $h = 0.68$m, Poisson's ratio $\nu = 0.2$, Young's modulus

$E = 2.11 \times 10^5$ Kg/cm^2 and density $\rho = 0.002$ Kg/cm^3. The base of the tank is subjected to vertical ground velocity pulses of the form

$$\frac{\partial u}{\partial t}(o,t) = \begin{cases} 1 \ , & 0 \leq t \leq t_o \\ 0 \ , & t > t_o \end{cases} \quad . \tag{3.43}$$

A first order longitudinal wave is generated by this boundary condition and higher order waves of the other types are induced due to the assumed homogeneous boundary conditions on the other field variables. These higher order waves produce effects at least two orders higher than the order of the generated wave. For axisymmetric transients these effects are usually negligible (and completely absent for small values of T) and therefore do not appreciably affect the peak response. Using equations (3.20) and (3.21) together with the corresponding boundary condition for the unit pulse solution, we obtain

$$A_1 = -1,\ B_1 = 0,\ C_1 = 0,\ D_1 = 0,$$

$$A_2 = -6.94 \times 10^{-6}s,\ B_2 = 0,\ C_2 = -3.50 \times 10^{-6},\ D_2 = 55.55 \times 10^{-6},$$

$$A_3 = -17.62 \times 10^{-12}s^2,\ B_3 = 2757 \times 10^{-12},\ C_3 = -24.52 \times 10^{-12}s,$$

$$D_3 = 385.16 \times 10^{-12}s, \text{ etc.} \tag{3.44}$$

Using equations (3.35), (3.37), (3.43) and (3.44) we can obtain the required transient solution. In Figure 5 we have plotted the response of the predominant strain $\frac{\partial u}{\partial s}$ with respect to T, the time after the arrival of the wavefront. The results for

$t_o = 10, 20, 30\ \mu$ secs together with that for $t_o \to \infty$ are shown. It must be remarked here that these series solutions begin to diverge at some value of $T > 53\ \mu$ secs.

The modified solutions were obtained by using the superposition technique with $t_o^* = 1\ \mu$ sec. For the range of T shown in Figure 5, we obtained perfect agreement between the series and modified solutions for the cases $t_o = 10, 20$ and $30\ \mu$ secs.

The results at other locations displayed similar behaviour. As the responses presented for the cases $t_o = 10$ and $20\ \mu$ secs decay approximately to zero, they could be used as test solutions in seeking the responses due to boundary loads with longer durations. Such a situation is presented below.

The ground motion resulting from a blast load has been determined by Awojobi and Sobaya [23] and also by Pekeris and Lifson [24]. We wish to obtain the response of our cylindrical tank when its base is subjected to this blast load. For the case r/H = 0.25 of Pekeris [24], the boundary condition due to the vertical ground velocity pulse is given by

$$\frac{\partial u}{\partial t}(0,t) = \begin{cases} A\ , & 0 \leq t \leq t_0 \\ 0\ , & t > t_o \end{cases}\ , \qquad (3.45)$$

while the boundary conditions on the other field variables are assumed to be homogeneous. In the above equation A is a constant. Considering the case $t_o = 2000\ \mu$ secs and the test solution with $t_o^* = 10\ \mu$ secs we obtain the modified solution for the strain $\frac{\partial u}{\partial s}$. This is shown in Figure 6 together with the corresponding series solution. As expected, the series solution begins to diverge beyond $T = 53$ μ secs. Analogous results were obtained at other locations.

3.4.3 Example 3 - Cylindrical Tank Subjected to Vertical Ground Acceleration Pulses

We now consider the tank of the previous example but the base being subjected to vertical ground acceleration pulses of the form

$$\frac{\partial^2 u}{\partial t^2}(0,t) = \begin{cases} 1 \,, & 0 \leq t \leq t_o \\ 0 \,, & t > t_o \end{cases} \,. \tag{3.46}$$

This boundary condition generates a second order longitudinal wave. The effects of the higher order waves, induced by the homogeneous boundary conditions on the other field variables, are negligible. Proceeding in a similar manner to that described above, we compute the series solutions for the predominant strain $\frac{\partial u}{\partial s}$. We wish to remark here that the coefficients for the corresponding unit pulse solution will be the same as before, provided we increase the subscripts by one and change the signs. The series solutions for the cases $t_o = 5, 10, 20$ and 30 μ secs and for the case $t_o \to \infty$ are shown in Figure 7, plotted with respect to T, the time after arrival of the wavefront at the location. As in the previous example all these solutions begin to diverge at some value of $T > 53$ μ secs.

The modified solutions were obtained by using the superposition technique with $t_o^* = 1\ \mu$ sec. For the range of T shown in Figure 7, we obtained perfect agreement between the series and modified solutions for all cases except for that with $t_o \to \infty$. Moreover, the responses for the cases $t_o = 5$, 10 and 20 μ secs decay to zero in the range of T considered. Hence they can be utilised as test solutions to obtain the response due to an acceleration boundary condition of longer duration.

In the solution of transient problems, the peak response is the important consideration [25]. For the case of a structure subjected to ground excitation due to an earthquake, Veletos et al [26] and Walker [27] consider the largest pulse from the accelerogram record and solve for the transient response due to this. Usually such pulses can be approximated by sine functions [26]. For the cylindrical tank subjected to such a ground acceleration pulse, the boundary condition is of the form

$$\frac{\partial^2 u}{\partial t^2}(0,t) = \begin{array}{ll} A \sin(\pi t/t_o) & , \; 0 \leq t \leq t_o \\ 0 & , \; t > t_o \end{array} \quad , \qquad (3.47)$$

where A is a constant. Considering the case $t_o = 2000\ \mu$ secs and utilising the test solution with $t_o^* = 20\ \mu$ secs, we obtained the modified solution for the strain $\frac{\partial u}{\partial s}$. The result is shown in Figure 8 where we can clearly observe the peak response. The procedure was repeated using test solutions with $t_o^* = 10\ \mu$ secs and $t_o^* = 5\ \mu$ secs. No appreciable change in the previous response curve was noted, thereby confirming the the plot in Figure 8.

3.4.4 Solutions at Different Locations

To obtain the responses at different locations in a structure we need test solutions at these locations. These test solutions as a rule have certain properties and display a particular pattern. In Figure 9 we illustrate some of the solutions obtained from example 2 at different locations. The wavefront ($T = 0$) values of all the test solutions depend on the first term in the series (3.35) or (3.37). In the case of cylindrical shells this term has the constant value of unity resulting in the same value of G_L^{-1} at $T = 0$ for all the solutions. This fact is observed in Figure 9 where all the curves start from the same point. For conical shells and for circular plates the first term in the series (3.35) or (3.37) decays as $(s_o/s)^{\frac{1}{2}}$ and the wavefront values of the test solutions at all locations can be determined if one such value is known. Moreover the test solutions will have jumps at $T = t_o^*$, which will be equal to their wavefront values. In Figure 9 the jumps AA', BB' and CC' are all equal to the constant wavefront value G_L^{-1} of the test solutions. The above observations become of use in determining test solutions. Finally the boundary load together with the test solutions yields the required responses by the superposition technique.

3.4.5 Effect of Thickness in a Cylindrical Shell

We now wish to study the effect of the thickness on the response of a cylindrical shell. In example 2 we increase the thickness keeping the radius constant and thereby obtain different h/a ratios. The test solutions with $t_o^* = 10\ \mu$ secs were computed for the predominant strain $\frac{\partial u}{\partial s}$ for the different ratios. In Figure 10, we illustrate these strain pulses, plotted with respect to T. We observe that the time taken for the response to decay to zero increases with increasing thickness. Moreover the slopes of the response curve decrease with increasing thickness and as a consequence decrease the magnitude of the strain reversal after the passage of the pulse. The pulse distortions shown in Figure 10 are a consequence of dispersion.

The decrease in the slope of the response curves with increase in thickness can be explained by considering the integrand $\bar{T}^A_{n-1}$ in equation (3.20), which is the transport equation for the case considered. The contributions to $\bar{T}^A_{n-1}$ are predominantly from the induction equation $(3.21)_3$ as can be observed from equation (3.44). The discontinuities D_n are determined by equations $(3.21)_3$, (3.34) and (3.17). The non zero coefficients d_{io} appearing in equation (3.17) depend on $1/h^2$ and the contribution to $\bar{T}^A_{n-1}$ from equation $(3.21)_3$ is decreased with increase in h. This will decrease the values of A_2 and A_3 determined by equation (3.20) and will cause the decrease in the slopes mentioned earlier. Although pulse distortion will not be eliminated due to the contributions from the other induction equations, it will be reduced for thick cylindrical shells.

3.4.6 Approximate Thin Rod Theories

In the example considered in section 3.4.1, the uniaxial theory was employed for dealing with longitudinal transients in a conical shell. Analogously the propagation of longitudinal transients in a cylindrical shell can be approximately treated by the various rod theories available. A brief discussion on the suitability of the rod theories for treating transient phenomena, will be in order at this stage.

For cylinders the elementary theory, where the non dispersive wave equation governs the propagation of longitudinal pulses, was the first to be used. According to this theory there will be no distortion of pulses and the response will be identical to the input pulse. In contrast, the elementary theory for a cone, referred to as the uniaxial theory, gives a dispersive equation due to the change in the cross-sectional area.

Experiments showed the distortion of pulses in cylinders and prompted the need for improved theories. The first improvement was to include the effects of radial inertia, as suggested by Rayleigh [28]. Love [29] incorporated this correction and presented the governing equation which is dispersive. However as this theory predicts instantaneous pulse propagation without a definite wavefront, it cannot account for the high frequency components in a transient. Mindlin and Herrman [30] included the effects of radial shear in addition to those of radial inertia and presented a more refined theory. The governing equations are both hyperbolic and dispersive giving two finite values for the wavefront speeds. Within its order of approximation, the Mindlin-Herrmann theory can account for all the frequencies in a transient. For a more detailed discussion on the above theories and related references we refer the reader to Graff [13].

The shell equations that we employed in this paper represent a theory two orders higher than that of Mindlin and Herrmann. These shell equations can be reduced to give those corresponding to the above mentioned rod theories by assigning appropriate values to the coefficients a_{io}, b_{io}, c_{io} and d_{io}.

CHAPTER IV

TRANSIENTS IN CYLINDRICAL SHELLS

4.1 Equations of Motion

In this chapter we consider the propagation of transients in linear, elastic, isotropic and homogeneous cylindrical shells subjected to boundary loads. The present theory contains the case of axi-symmetric transients in a cylindrical shell as a special case.

As before, we utilise Naghdi's equations [1], [14] which are derived from the Cosserat theory and which include the effects of transverse shear, transverse normal stress and strain and rotatory inertia. We denote the axial (x), circumferential (θ) and the radial displacements of the shell mid-surface by u, v, w respectively and the rotations of the normal to the mid-surface about the circumferential and axial directions by ψ_x, ψ_θ respectively and the transverse normal strain by ψ_z. Since we are considering propagation in the axial direction and the complete shell in the circumferential direction, we express the field variables in the form of Fourier series in θ as

$$
\begin{aligned}
u &= \sum_{m=o}^{\infty} u_m \cos m\theta \ , \quad \psi_x = \sum_{m=o}^{\infty} \psi_{xm} \cos m\theta \ , \quad w = \sum_{m=o}^{\infty} w_m \cos m\theta \\
\psi_z &= \sum_{m=o}^{\infty} \psi_{zm} \cos m\theta \ , \quad v = \sum_{m=o}^{\infty} v_m \sin m\theta \ , \quad \psi_\theta = \sum_{m=o}^{\infty} \psi_{\theta m} \sin m\theta \ .
\end{aligned}
\tag{4.1}
$$

The displacement equations of motion now take the form

$$\frac{\partial^2 u_m}{\partial x^2} - \frac{1}{G_L^2}\frac{\partial^2 u_m}{\partial t^2} = \sum_{i=1}^{12} a_{im} V_{im} \quad , \tag{4.2}$$

$$\frac{\partial^2 \psi_{xm}}{\partial x^2} - \frac{1}{G_B^2}\frac{\partial^2 \psi_{xm}}{\partial t^2} = \sum_{i=1}^{12} b_{im} V_{im} \quad , \tag{4.3}$$

$$\frac{\partial^2 w_m}{\partial x^2} - \frac{1}{G_K^2}\frac{\partial^2 w_m}{\partial t^2} = \sum_{i=1}^{12} c_{im} V_{im} \quad , \tag{4.4}$$

$$\frac{\partial^2 \psi_{zm}}{\partial x^2} - \frac{1}{{G_S}^2}\frac{\partial^2 \psi_{zm}}{\partial t^2} = \sum_{i=1}^{12} d_{im} V_{im} \quad , \tag{4.5}$$

$$(1+\alpha/a^2)\frac{\partial^2 v_m}{\partial x^2} - \frac{1}{G_T^2}\frac{\partial^2 v_m}{\partial t^2} - \frac{\alpha}{a}\frac{\partial^2 \psi_{\theta m}}{\partial x^2} = \sum_{i=1}^{12} e_{im} V_{im} \quad , \tag{4.6}$$

$$\frac{\partial^2 \psi_{\theta m}}{\partial x^2} - \frac{1}{G_T^2}\frac{\partial^2 \psi_{\theta m}}{\partial t^2} - \frac{1}{a}\frac{\partial^2 v_m}{\partial x^2} = \sum_{i=1}^{12} f_{im} V_{im} \quad . \tag{4.7}$$

In the above equations a is the radius of the cylinder. The wavefront speeds are given by

$$G_L^2=C(1-\nu)/(1-2\nu)\rho, G_B^2=C/\rho, G_K^2=\alpha_3/\rho, G_S^2=\alpha_8/\rho\alpha, G_T^2=C(1-\nu)/2\rho. \tag{4.8}$$

The quantities V_{im} are given by

$$\begin{aligned} V_{1m} &= \frac{\partial u_m}{\partial x} , \quad V_{2m} = u_m , \quad V_{3m} = \frac{\partial \psi_{xm}}{\partial x} , \quad V_{4m} = \psi_{xm} , \\ V_{5m} &= \frac{\partial w_m}{\partial x} , \quad V_{6m} = w_m , \quad V_{7m} = \frac{\partial \psi_{zm}}{\partial x} , \quad V_{8m} = \psi_{zm} , \\ V_{9m} &= \frac{\partial v_m}{\partial x} , \quad V_{10m} = v_m , \quad V_{11m} = \frac{\partial \psi_{\theta m}}{\partial x} , \quad V_{12m} = \psi_{\theta m} . \end{aligned} \tag{4.9}$$

The constant coefficients a_{im}, b_{im}, c_{im}, d_{im}, e_{im}, f_{im} (i=1-12) which involve the material and geometric parameters of the cylinder are given in Appendix II. The other quantities were defined earlier. By setting $m = 0$ equations (4.2)-(4.7) will uncouple to give those corresponding to torsionless axi-symmetric and torsional motions.

Equations (4.2)-(4.7) being dispersive [2], will cause transient pulses to suffer distortion and the phase velocities of time-harmonic waves to be frequency dependent. However, finite wavefront speeds for transients and bounded phase velocities for time-harmonic waves are assured due to the hyperbolic nature of these equations [3]. Thus the displacement equations of motion presented above are amenable to solution by the method of discontinuity analysis or by the method of characteristics.

4.2 Method of Solution

As discussed in the previous chapter, the first step in obtaining a transient solution by our method is the determination of the unit pulse solution. We defined the unit pulse solution as the solution due to a step boundary pulse of unit magnitude. The Duhamel integral and the specified boundary condition then give us the required transient solution. In order to determine the unit pulse solution, we need to determine the displacement discontinuities of all order at the wavefront, and represent the solution in the form of a Taylor series expansion behind the wavefront [4]. The equations that determine these discontinuities are called the transport-induction equations and are generated much more easily by the Karal-Keller technique [10] than by the method of discontinuity analysis.

To this end we assume time-harmonic solutions to equations (4.2)-(4.7) in the form

$$
\begin{aligned}
u_m &= e^{i\omega(S-t)} \sum_{n=1}^{\infty} \frac{A_n}{(i\omega)^n}, \quad \psi_{xm} = e^{i\omega(S-t)} \sum_{n=1}^{\infty} \frac{B_n}{(i\omega)^n}, \\
w_m &= e^{i\omega(S-t)} \sum_{n=1}^{\infty} \frac{C_n}{(i\omega)^n}, \quad \psi_{zm} = e^{i\omega(S-t)} \sum_{n=1}^{\infty} \frac{D_n}{(i\omega)^n}, \\
v_m &= e^{i\omega(S-t)} \sum_{n=1}^{\infty} \frac{E_n}{(i\omega)^n}, \quad \psi_{\theta m} = e^{i\omega(S-t)} \sum_{n=1}^{\infty} \frac{F_n}{(i\omega)^n}
\end{aligned}
\tag{4.10}
$$

where S is the phase function, ω the circular frequency and the amplitude functions of the time-harmonic series are given by [5],

$$
\begin{aligned}
A_n &= (-1)^n [u^H_{m,n}], \quad B_n = (-1)^n [\psi^H_{xm,n}], \quad C_n = (-1)^n [w^H_{m,n}] \\
D_n &= (-1)^n [\psi^H_{zm,n}], \quad E_n = (-1)^n [v^H_{m,n}], \quad F_n = (-1)^n [\psi^H_{\theta m,n}] .
\end{aligned}
\tag{4.11}
$$

In the above equations $[\ ]$ indicates the discontinuity or jump of the argument across the wavefront, the comma followed by n denotes n^{th} order time derivative and the superscript H denotes the unit pulse solution. On substituting equations (4.10) into equations (4.2)-(4.7) and formally requiring that the coefficients of powers of $(i\omega)$ separately vanish, we obtain the recurrence relations for $n \geq 1$ as

$$A_n(1-G^2/G_L^2) + 2G\frac{dA_{n-1}}{dx} = G^2T^A_{n-2} \quad , \tag{4.12}$$

$$B_n(1-G^2/G_B^2) + 2G\frac{dB_{n-1}}{dx} = G^2T^B_{n-2} \quad , \tag{4.13}$$

$$C_n(1-G^2/G_K^2) + 2G\frac{dC_{n-1}}{dx} = G^2T^C_{n-2} \quad , \tag{4.14}$$

$$D_n(1-G^2/G_S^2) + 2G\frac{dD_{n-1}}{dx} = G^2T^D_{n-2} \quad , \tag{4.15}$$

$$E_n(1+\alpha/a^2-G^2/G_T^2)+2G(1+\alpha/a^2)\frac{dE_{n-1}}{dx}-(\alpha/a)(F_n+2G\frac{dF_{n-1}}{dx})=G^2T^E_{n-2} . \tag{4.16}$$

$$F_n(1-G^2/G_T^2) + 2G\frac{dF_{n-1}}{dx} - (E_n+2G\frac{dE_{n-1}}{dx})/a = G^2T^F_{n-2} \ . \tag{4.17}$$

In equations (4.12)-(4.17), G is the wavefront speed, related to S in the form

$$\frac{dS}{dx} = 1/G \tag{4.18}$$

and

$$\begin{aligned} T^A_{n-2} = &-\frac{d^2A_{n-2}}{dx^2} + a_{2m}A_{n-2} + a_{5m}(\frac{C_{n-1}}{G} + \frac{dC_{n-2}}{dx}) \\ &+ a_{7m}(\frac{D_{n-1}}{G} + \frac{dD_{n-2}}{dx}) + a_{9m}(\frac{E_{n-1}}{G} + \frac{dE_{n-2}}{dx}) \quad , \end{aligned} \tag{4.19}$$

$$\begin{aligned} T^B_{n-2} = &-\frac{d^2B_{n-2}}{dx^2} + b_{4m}B_{n-2} + b_{5m}(\frac{C_{n-1}}{G} + \frac{dC_{n-2}}{dx}) \\ &+ b_{9m}(\frac{E_{n-1}}{G} + \frac{dE_{n-2}}{dx}) + b_{11m}(\frac{F_{n-1}}{G} + \frac{dF_{n-2}}{dx}) \quad , \end{aligned} \tag{4.20}$$

$$T^C_{n-2} = -\frac{d^2C_{n-2}}{dx^2} + c_{1m}\left(\frac{A_{n-1}}{G} + \frac{dA_{n-2}}{dx}\right) + c_{3m}\left(\frac{B_{n-1}}{G} + \frac{dB_{n-2}}{dx}\right)$$

$$+ c_{6m}C_{n-2} + c_{8m}D_{n-2} + c_{10m}E_{n-2} + c_{12m}F_{n-2}\ , \tag{4.21}$$

$$T^D_{n-2} = -\frac{d^2D_{n-2}}{dx^2} + d_{1m}\left(\frac{A_{n-1}}{G} + \frac{dA_{n-2}}{dx}\right) + d_{6m}C_{n-2}$$

$$+ d_{8m}D_{n-2} + d_{10m}E_{n-2}\ , \tag{4.22}$$

$$T^E_{n-2} = -(1+\alpha/a^2)\frac{d^2E_{n-2}}{dx^2} + \frac{\alpha}{a}\frac{d^2F_{n-2}}{dx^2} + e_{1m}\left(\frac{A_{n-1}}{G} + \frac{dA_{n-2}}{dx}\right)$$

$$+ e_{3m}\left(\frac{B_{n-1}}{G} + \frac{dB_{n-2}}{dx}\right) + e_{6m}C_{n-2} + e_{8m}D_{n-2} \tag{4.23}$$

$$+ e_{10m}E_{n-2} + e_{12m}F_{n-2}\ ,$$

$$T^F_{n-2} = -\frac{d^2F_{n-2}}{dx^2} + \frac{1}{a}\frac{d^2E_{n-2}}{dx^2} + f_{3m}\left(\frac{B_{n-1}}{G} + \frac{dB_{n-2}}{dx}\right)\ ,$$

$$+ f_{6m}C_{n-2} + f_{10m}E_{n-2} + f_{12m}F_{n-2}\ . \tag{4.24}$$

We have used the fact that certain coefficients are zero in writing down the right hand sides of the above equations.

Considering first order waves and setting n=1 in equations (4.12)-(4.17) will yield,

$$(G^2-G_L^2)A_1 = 0,\ (G^2-G_B^2)B_1 = 0,\ (G^2-G_K^2)C_1 = 0,\ (G^2-G_S^2)D_1 = 0$$

$$\{G^2-(1+\alpha/a^2)G_T^2\}E_1 + (\alpha/a)G_T^2F_1 = 0,\ (G^2-G_T^2)F_1 + G_T^2E_1 = 0\ . \tag{4.25}$$

From the above set of equations we can obtain the classification [14], speeds and propagation conditions for first order waves. Moreover substituting the appropriate speed G in turn, into equations (4.12)-(4.17) with $n \geq 2$, we obtain the transport-induction equations for each wave type. However equations (4.16) and (4.17) are coupled and have to be solved simultaneously. As a result we obtain a coupled transport equation for the waves pertaining to these two equations and coupled induction equations for the other wave types. We present below the results for each case.

(i) *Longitudinal Wave*

$$G = G_L,\ A_1 \neq 0,\ B_1 = 0,\ C_1 = 0,\ D_1 = 0,\ E_1 = 0,\ F_1 = 0\ . \tag{4.26}$$

$$A_n(x) = A_n(x_o) + \frac{G}{2}\int_{x_o}^{x} T^A_{n-1}(\tau)\,d\tau\ . \tag{4.27}$$

$$B_n = P^B_n,\ C_n = P^C_n,\ D_n = P^D_n,\ E_n = P^E_n,\ F_n = P^F_n\ . \tag{4.28}$$

(ii) *Bending Wave*

$$G = G_B,\ B_1 \neq 0,\ A_1 = 0,\ C_1 = 0,\ D_1 = 0,\ E_1 = 0,\ F_1 = 0\ . \tag{4.29}$$

$$B_n(x) = B_n(x_o) + \frac{G}{2}\int_{x_o}^{x} T^B_{n-1}(\tau)\,d\tau\ . \tag{4.30}$$

$$A_n = P^A_n,\ C_n = P^C_n,\ D_n = P^D_n,\ E_n = P^E_n,\ F_n = P^F_n\ . \tag{4.31}$$

(iii) *Kink Wave*

$$G = G_K,\ C_1 \neq 0,\ A_1 = 0,\ B_1 = 0,\ D_1 = 0,\ E_1 = 0,\ F_1 = 0\ . \tag{4.32}$$

$$C_n(x) = C_n(x_o) + \frac{G}{2}\int_{x_o}^{x} T^C_{n-1}(\tau)\,d\tau\ . \tag{4.33}$$

$$A_n = P^A_n,\ B_n = P^B_n,\ D_n = P^D_n,\ E_n = P^E_n,\ F_n = P^F_n\ . \tag{4.34}$$

(iv) *Squeeze-Gradient Wave*

$$G = G_S,\ D_1 \neq 0,\ A_1 = 0,\ B_1 = 0,\ C_1 = 0,\ E_1 = 0,\ F_1 = 0\ . \tag{4.35}$$

$$D_n(x) = D_n(x_o) + \frac{G}{2}\int_{x_o}^{x} T^D_{n-1}(\tau)\,d\tau\ . \tag{4.36}$$

$$A_n = P^A_n,\ B_n = P^B_n,\ C_n = P^C_n,\ E_n = P^E_n,\ F_n = P^F_n\ . \tag{4.37}$$

(v) *Transverse and Twisting Waves*

$$G = G_T\{1+\alpha/2a^2 \pm (4\alpha/a^2+\alpha^2/a^4)^{\frac{1}{2}}/2\}\ , \tag{4.38}$$

$$E_1 \neq 0,\ F_1 \neq 0,\ A_1 = 0,\ B_1 = 0,\ C_1 = 0,\ D_1 = 0\ .$$

$$K_1 = G^2-(1+\alpha/a^2)G_T^2,\ K_2 = \alpha G_T^2/a,\ K_3 = K_2/\alpha,\ K_4 = G^2-G_T^2\ , \tag{4.39}$$

$$K_5 = (1+\alpha/a^2)K_4 + K_2/a,\ K_6 = \alpha K_4/a + K_2\ . \tag{4.40}$$

$$L_n(x) = L_n(x_o) + \frac{G}{2}\int_{x_o}^{x}\{K_4T^E_{n-1}(\tau)-K_2T^F_{n-1}(\tau)\}d\tau\ , \tag{4.41}$$

where

$$L_n = K_5E_n - K_6F_n\ .$$

$$E_n = K_2[L_n + (K_6/K_2)\{T^E_{n-2} - \frac{2}{G}(1+\alpha/a^2)\frac{dE_{n-1}}{ds} + (2\alpha/Ga)\frac{dF_{n-1}}{ds}\}]/(K_2K_5+K_1K_6) \quad . \tag{4.42}$$

$$F_n = (K_5E_n - L_n)/K_6 \quad . \tag{4.43}$$

$$A_n = P^A_n, \; B_n = P^B_n, \; C_n = P^C_n, \; D_n = P^D_n \quad . \tag{4.44}$$

There will be two separate solutions corresponding to the two values of G obtained from equation $(4.38)_1$. These two solutions have to be superposed taking into account the time lag that exists between them.

In the above sets of equations P^A_n, P^B_n, P^C_n, P^D_n, P^E_n and P^F_n are functions of the wave speed and are given by

$$P^A_n = \frac{G\,G_L^2}{G_L^2-G^2}\left(GT^A_{n-2} - 2\frac{dA_{n-1}}{dx}\right) \quad , \tag{4.45}$$

$$P^B_n = \frac{G\,G_B^2}{G_B^2-G^2}\left(GT^B_{n-2} - 2\frac{dB_{n-1}}{dx}\right) \quad , \tag{4.46}$$

$$P^C_n = \frac{G\,G_K^2}{G_K^2-G^2}\left(GT^C_{n-2} - 2\frac{dC_{n-1}}{dx}\right) \quad , \tag{4.47}$$

$$P^D_n = \frac{G\,G_S^2}{G_S^2-G^2}\left(GT^D_{n-2} - 2\frac{dD_{n-1}}{dx}\right) \quad , \tag{4.48}$$

$$P^E_n = (K_{10}R^E_{n-1} - K_8R^F_{n-1})/(K_7K_{10} - K_8K_9) \quad , \tag{4.49}$$

$$P^F_n = (R^E_{n-1} - K_7E_n)/K_8 \quad , \tag{4.50}$$

where K_7, K_8, K_9, K_{10}, R^E_{n-1}, R^F_{n-1} are also functions of G and are given by,

$$K_7 = (1+\alpha/a^2)/G^2 - 1/G_T^2 \ , \ K_8 = -\alpha/aG^2$$

$$K_9 = K_8/\alpha \ , \ K_{10} = 1/G^2 - 1/G_T^2 \ , \tag{4.51}$$

$$R^E_{n-1} = T^E_{n-2} - \frac{2}{G}(1+\alpha/a^2)\frac{dE_{n-1}}{dx} + \frac{2\alpha}{aG}\frac{dF_{n-1}}{dx} \ , \tag{4.52}$$

$$R^E_{n-1} = T^E_{n-2} + \frac{2}{aG}\frac{dE_{n-1}}{dx} - \frac{2}{G}\frac{dF_{n-1}}{dx} \ . \tag{4.53}$$

For each wave type G denotes the eigen value corresponding to the eigen vector $(A_1,B_1,C_1,D_1,E_1,F_1)$. The equation with the integral is the solution to the transport equation and the P^S_n represent the induction equations. The boundary value of x is denoted by x_o. The boundary conditions and equation (4.11) together with the appropriate transport-induction equations will determine the required discontinuities. The corresponding unit pulse solution U^H is then given by the Taylor series [5]

$$U^H = \sum_{n=1} [\underset{\sim}{U}{}^H_{,n}]\underset{\sim}{<}t-S>^n/n! \ , \tag{4.54}$$

with

$$S = S(x_o) + (x-x_o)/G \ , \tag{4.55}$$

where U stands for any one of the field variables u_m, ψ_{xm}, w_m, ψ_{zm}, v_m or $\psi_{\theta m}$, and $< > = 0$, if the argument is negative. The required transient solution is then given by [9]

$$U = \int_0^t \frac{\partial U^H(t-\tau)}{\partial t} f(\tau)\,d\tau \ , \tag{4.56}$$

where f(t) is the time dependance of the boundary condition.

Finally the solutions for all the applicable values of m, depending on the boundary condition, have to be superposed.

The results for second and higher order waves could be obtained in an analogous manner by starting with the appropriate value of n in equations (4.10)-(4.17).

Later on in this chapter, in section (4.4), we present some numerical examples to illustrate our method of solution.

4.3 Approximate Thin Rod Theories

The propagation of transients in cylindrical shells can also be approximately treated by the various rod theories [13]. Hence it is of interest to discuss the suitability of these rod theories in treating transient phenomena. There are three different types of wave motion in thin rods; these being classed as longitudinal, torsional and flexural. In shells, there are motions corresponding to each of the above types and the appropriate equations of motion can be obtained from equations (4.2)-(4.7). By setting $m = 0$, the shell equations uncouple to give the equations for axi-symmetric and torsional motions. On the other hand, if we set $m = 1$, we obtain the shell equations for flexural motion. The propagation of longitudinal waves in a rod corresponds to that of axi-symmetric waves in shells and this was discussed in the previous chapter. In this section we propose to discuss briefly the other two types of wave motion.

Whether we use the strength of materials approach or the general elasticity relations, we arrive at the non dispersive wave equation, as the one governing the torsional mode in a rod. Thus a torsional pulse will propagate undistorted with a finite wavefront speed and torsional harmonic waves will have bounded phase velocities. As the wave equation is amenable to solution by various methods, we do not attempt to solve it in this chapter. However, we wish to remark that our shell equations, (4.6) and (4.7) with $m = 0$, are dispersive. This is due to the fact that they were derived from the Cosserat theory. The propagation of non axi-symmetric torsional transients can also be treated by using the results presented in the previous section, together with appropriate boundary conditions. In this case, $m \neq 0$ and there will be coupling with all the possible wave types. In the next section we present a numerical example which will illustrate the distortion of a non axi-symmetric pulse.

The Euler-Bernoulli theory derived from the strength of materials approach was the first to describe the flexural motion in a rod. The resulting equation is dispersive but predicts instantaneous pulse propagation without a distinct wavefront and unbounded phase velocities for high frequency time harmonic waves. Hence this theory cannot account for the high frequency components in a transient. Rayleigh [28] incorporated the correction for rotatory inertia and presented a dispersive equation which gives a finite wavefront speed for the bending wave. The Rayleigh theory neglects the shear correction and hence an infinite wavefront speed for the shear or kink wave is predicted. If the shear correction is included without the correction for rotatory inertia, the resulting equation will predict finite and infinite wavefront speeds for the kink and bending waves respectively. In either case the mathematical model does not describe the motion completely and the high frequency components in a transient are not completely accounted for. Timoshenko [31] included both the corrections mentioned above and presented a theory with two coupled second order equations. According to this theory, we obtain finite wavefront speeds for both the bending and kink waves. Hence the Timoshenko theory can satisfactorily account for the high frequency components of the transients in the flexural motion. Equations (4.3) and (4.4) can be reduced to the Timoshenko equations by assigning $m = 1$ and then appropriate values to the coefficients b_{i1} and c_{i1}.

In the next section we first solve a Timoshenko beam problem and validate our method by comparing the solution with an existing one. We then treat the flexural and torsional problems in a cylindrical shell. For the former problem the results obtained from the shell and beam theories are compared.

4.4 Numerical Examples and Discussion

As we had dealt with the axi-symmetric motion in cylinders in the previous chapter, herein we confine our attention to the flexural and torsional motions.

4.4.1. Example 1: -Transverse Impact of a Timoshenko Beam

We consider a semi infinite beam subjected to a transverse step velocity and a zero bending moment at the end. The appropriate boundary conditions for the Timoshenko beam equations are

$$\frac{\partial w_1}{\partial t}(0,t) = H(t) \quad , \quad \frac{\partial \psi_{x1}}{\partial x}(0,t) = 0 \tag{4.57}$$

This problem has been solved by Boley and Chao [17] using Laplace transforms. Using equations $(4.11)_2$, $(4.11)_3$ and (4.29)-(4.34) we obtain in a recursive manner.

$$\begin{aligned} &B_1=0, B_2=0.26, B_3=-0.034x_1, B_4=0.0022x_1^2+0.077, \\ &C_1=-1, C_2=0.13x_1, C_3=-0.0085x_1^2, C_4=0.00037x_1^2+0.024x_1, \text{etc.} \end{aligned} \tag{4.58}$$

for the first order kink wave and

$$\begin{aligned} &B_1^1=0, B_2^1=-0.26, B_3^1=-0.11x_1, B_4^1=-0.013x_1+0.0065, \\ &C_1^1=0, C_2^1=0, C_3^1=0.22, C_4^1=0.052x_1, C_5^1=0.006x_1^2+0.097, \text{etc.} \end{aligned} \tag{4.59}$$

for the higher order bending wave. In the above two equations $x_1 = x/\sqrt{\alpha}$ where α was defined previously. Using equations $(4.11)_3$, (4.54) and (4.55) we obtain the unit pulse solution, which is the required transient solution for this case.

In Figure 11 we have plotted the variation of the velocity $\frac{\partial w}{\partial t}$ with position and compare the results with those of Boley and Chao. The time of observation is given by $t_1 = tG_B/\sqrt{\alpha} = 5$. The bending wave is the faster of the two waves and its wavefront is at $x_1 = 5$ in the figure. The velocity increases behind the wavefront, until the slower moving kink wave is encountered. At the wavefront of the kink wave there is a discontinuity in the velocity equal in magnitude to the input velocity at the boundary. Behind this wavefront the contributions due to both the waves are superposed. We observe that our solution obtained by using a few terms in the series (4.54) compares quite well with that of Boley and Chao. Analogous comparisons were obtained for the shear force Q, demonstrating the validity of the method of solution.

4.4.2. Ground Excitation

An important application of non axi-symmetric wave propagation is found in the case of a cylindrical shell structure subjected to ground excitation, resulting from blast loads, earthquakes, etc. Such ground waves are generally incident at an angle with the vertical and can be decomposed into their vertical and horizontal components. The vertical ground excitation gives rise to axi-symmetric wave motion and this has been treated in the previous chapter.

The horizontal ground excitation will give rise to flexural and torsional wave motions. Referring to Figure 12, if we denote the ground displacement by u_G, then the boundary conditions for the generation of n^{th} order waves are given by

$$\frac{\partial^n w}{\partial t^n}(0,t) = \frac{\partial^n u_G}{\partial t^n} \cos\theta \ , \ \frac{\partial^n v}{\partial t^n}(0,t) = - \frac{\partial^n u_G}{\partial t^n} \sin \theta \ . \quad (4.60)$$

Thus in general the kink wave and the transverse-twisting waves are generated due to horizontal ground excitation. In the examples that follow, the boundary conditions on the field variables v, ψ_x and ψ_z are assumed to be zero, while the boundary conditon on ψ_θ is coupled to that on v[1] and is given by

$$\psi_\theta(0,t) = v(0,t)/a \; . \tag{4.61}$$

From equations (4.1) and (4.60) we observe that only the case m = 1, need to be considered in solving problems due to ground excitation. Under the above conditions the generation of the kink and transverse-twisting waves are referred to as the flexural and torsional problems respectively.

In example 2 we consider the flexural problem due to a first order kink wave and in example 3 we deal with the torsional problem.

4.4.3. Example 2: - Cylindrical Tank Subjected to Horizontal Ground Excitation - the Flexural Problem

We consider the cylindrical tank discussed in the previous chapter with its base subjected to a step velocity resulting from horizontal ground excitation. The only nonhomogeneous boundary condition for the flexural problem is

$$\frac{\partial w_1}{\partial t}(0,t) = H(t) \; , \tag{4.62}$$

where we have assumed the horizontal ground velocity to be the Heaviside unit function. The resulting unit pulse solution can be used to obtain the transient solutions due to other boundary conditions with the aid of the Duhamel integral. Using equation (4.11) and the transport-induction equation for the first order kink wave we obtain

$$
\begin{aligned}
&A_1=0,\ A_2=-0.30\times10^{-6},\ A_3=0.03\times10^{-6}x,\ A_4=-(13\times10^{-12}x^2+0.02\times10^{-6}),\\
&B_1=0,\ B_2=-718\times10^{-6},\ B_3=0.65\times10^{-6}x,\ B_4=-(312\times10^{-12}x^2+0.18\times10^{-6}),\\
&C_1=-1,\ C_2=359\times10^{-6}x,\ C_3=-0.16\times10^{-6}x^2,\ C_4=51\times10^{-12}x^3+0.08\times10^{-6}x,\\
&D_1=0,\ D_2=0,\ D_3=0.71\times10^{-6}, \qquad (4.63)\\
&E_1=0,\ E_2=0,\ E_3=0.44\times10^{-6},\\
&F_1=0,\ F_2=0,\ F_3=0.14\times10^{-6},\ \text{etc.}
\end{aligned}
$$

In order to satisfy the homogeneous boundary conditions on the other field variables, we observe that higher order waves of the other types are induced. The predominant higher order wave is the bending wave as seen from the above results, and it travels faster than the lower order kink wave. Proceeding in an analogous manner, for the second order bending wave we obtain

$$
\begin{aligned}
&A_1^1=0,\ A_2^1=0,\ A_3^1=0,\\
&B_1^1=0,\ B_2^1=718\times10^{-6},\ B_3^1=0.45\times10^{-6}x,\ B_4^1=(0.00014x^2+0.03)10^{-6},\\
&C_1^1=0,\ C_2^1=0,\ C_3^1=17\times10^{-6},\ C_4^1=0.01\times10^{-6}x,\\
&D_1^1=0,\ D_2^1=0, \qquad (4.64)\\
&E_1^1=0,\ E_2^1=0,\ E_3^1=0.11\times10^{-6},\\
&F_1^1=0,\ F_2^1=0,\ F_3^1=0.32\times10^{-6},\ \text{etc.}
\end{aligned}
$$

Using equations (4.54), (4.55), (4.63) and (4.64) we compute the unit pulse solution. In Figure 13 the displacement w_1 at x= 30.5 cms is shown with respect to time after arrival of the bending wave. The corresponding displacement obtained by using the Timoshenko beam theory, is also shown. We observe that the contribution from the bending wave is neglibible for the beam and very small for the shell, prior to the arrival of the kink wave. The arrival of this wave at the particular location in the cylinder, is at K and K' according to the shell and beam theories respectively. The time lag is due to the slight difference in the wavefront speeds in the two theories. After the arrival of the kink wave, the contributions from both waves are superposed. The effect of the higher order bending wave becomes appreciable with increasing time.

4.4.4. Example 3: - Cylindrical Tank Subjected to Horizontal Ground Excitation - the Torsional Problem

In this example we treat the torsional problem for the cylindrical tank discussed earlier. We present the test solutions for the predominant strain due to first and second order transverse-twisting waves. If the test solutions are known, then they could be utilised to obtain the solutions corresponding to other boundary conditions. From equations (4.60) and (4.61) the non-homogeneous boundary conditions for the torsional problem are

$$\frac{\partial^n v_1}{\partial t^n}(0,t) = a\frac{\partial^n \psi_{\theta 1}}{\partial t^n} = \begin{matrix} 1, & 0 \leq t \leq t_o^* \\ 0, & t > t_o^* \end{matrix} \quad , \tag{4.65}$$

where we have assumed a step ground velocity (n=1) and a step ground acceleration (n=2) pulse. First and second order transverse-twisting waves are generated for n = 1 and n = 2 respectively, due to the above boundary condition. Considering the value of G = 0.1874 cms/μ sec in equation $(4.38)_1$ and using equations (4.38)-(4.44) we obtain in a recursive manner

$$
\begin{aligned}
&A_1=0,\ A_2=45\times10^{-6},\ A_3=-0.015\times10^{-6}x,\ A_4=0.013\times10^{-6}-1\times10^{-12}x^2,\\
&B_1=0,\ B_2=-10\times10^{-6},\ B_3=-0.003\times10^{-6}x,\ B_4=-0.23\times10^{-6}x^2-0.31\times10^{-6},\\
&C_1=0,\ C_2=0,\ C_3=0.21\times10^{-6}x,\\
&D_1=0,\ D_2=0,\ D_3=-0.0007\times10^{-6},\\
&E_1=0.503,\ E_2=170\times10^{-6}x,\ E_3=0.03\times10^{-6}x^2-36\times10^{-6},\\
&E_4=1.27\times10^{-12}x^3-0.002\times10^{-6}x,\\
&F_1=0.117,\ F_2=39\times10^{-6}x,\ F_3=0.006\times10^{-6}x^2+82\times10^{-6},\\
&F_4=0.34\times10^{-12}x^3+0.0007\times10^{-6}x,\ \text{etc.}
\end{aligned}
\tag{4.66}
$$

for the unit pulse solution corresponding to the velocity boundary condition. The coefficients for the acceleration boundary condition can be obtained from the above set by merely increasing the subscript values by one and by changing the signs. Using equations (4.54)-(4.56) and equations (4.65), (4.66) we can obtain the transient solutions for both boundary conditions. For $t_o^* = 1,2,5$ μ secs and $t_o^* \to \infty$, the predominant strain $\varepsilon_{\theta x} = \frac{1}{2}(\frac{\partial u}{\partial \theta} + \frac{\partial v}{\partial x})$ was calculated and the results are shown in Figures 14 and 15. The appropriate response curves in these figures could be used as test solutions to obtain the response due to ground excitations as in the previous chapter.

Analogous results were obtained for the solutions at other locations and for the solutions corresponding to the other value of G(=0.1899 cms/μ sec) in equation $(4.38)_1$.

APPENDIX I

The coefficients appearing in equations (3.1)-(3.4) are defined as follows:

$a_{10} = -1/s$, $a_{20} = (1+F)/s^2$, $a_{30} = -\nu F\tan\beta$, $a_{40} = -F\tan\beta/s$,
$a_{50} = \nu\ \mathrm{ot}\beta/(1-\nu)s$, $a_{60} = a_{20}\cot\beta$, $a_{70} = -\nu/(1-\nu)$, $a_{80} = 0$.

$b_{10} = \nu\cot\beta/s^2$, $b_{20} = -(1+\nu)\cot\beta/s^2$, $b_{30} = -1/s$,
$b_{40} = 1/s^2+\alpha_3/\alpha C$, $b_{50} = \alpha_3/\alpha C-\nu\cot\beta^2/s^2$, $b_{60} = -b_{20}\cot\beta$,
$b_{70} = 0$, $b_{80} = 0$.

$c_{10} = -\nu(1-\nu)C\cot\beta/(1-2\nu)\alpha_3 s$, $c_{20} = -\{(1-\nu)^2/(1-\nu)+H\}C\cot\beta/\alpha_3 s^2$,
$c_{30} = 1-C\nu H/\alpha_3$, $C_{40} = -(1-CH/\alpha_3)/s$, $c_{50} = -1/s$, $c_{60} = -c_{20}\cot\beta$,
$c_{70} = 0$, $c_{80} = c_{10}$.

$d_{10} = C\nu(1-\nu)/(1-2\nu)\alpha_8$, $d_{20} = d_{10}/s$, $d_{30} = 0$, $d_{40} = 0$,
$d_{50} = 0$, $d_{60} = -d_{20}\cot\beta$, $d_{70} = -1/s$, $d_{80} = (1-\nu)d_{10}/\nu$.

In the above expressions, β is the semi-vertical angle of the generator, $F = (1-2\nu)H/(1-\nu)^2$, $H = \alpha\cot^2\beta/s^2$. In this thesis α_3 and α_8 are assumed to have the values $5E/12(1+\nu)$ and $7E\alpha/20(1+\nu)$. For a conical shell, the radius r at any section is given by $r = s\sin\beta$, $s \neq 0$.

For a cylindrical shell, $\beta = 0$ and we have to substitute $s\sin\beta = a$, $\cos\beta = 1$.

For a circular plate, $\beta = \frac{\Pi}{2}$ and we have $s = r$.

APPENDIX II

The non zero coefficients appearing in equations (4.2)-(4.7) are defined as follows:

$a_{2m} = (1-2\nu)m^2/2(1-\nu)a^2$, $a_{5m} = \nu/(1-\nu)a$, $a_{7m} = \mp\nu/(1-\nu)$,
$a_{9m} = -m/2(1-\nu)a$.

$b_{4m} = \alpha_3/C\alpha+(1-\nu)m^2/2a^2$, $b_{5m} = \alpha_3/C\alpha-\nu/a^2$,
$b_{9m} = (1+\nu)m/2a^2$, $b_{11m} = -(1+\nu)m/2a$.

$c_{1m} = -C\nu(1-\nu)/\alpha_3(1-2\nu)a$, $c_{3m} = C\alpha\nu/\alpha_3 a^2-1$,
$c_{6m} = \{m^2+C(1-\nu)^2/\alpha_3(1-2\nu)+C\alpha/\alpha_3 a^2\}/a^2$, $c_{8m} = c_{1m}$,
$c_{10m} = -m\{1+C(1+\nu)^2/\alpha_3(1-2\nu)+C\alpha/\alpha_3 a^2\}/a^2$, $c_{12m} = m(C\alpha/\alpha_3 a^2-1)/a$.

$d_{1m} = C\nu(1-\nu)/\alpha_8(1-2\nu)$, $d_{6m} = -d_{1m}/a$,
$d_{8m} = m^2/a^2+C(1-\nu)^2/\alpha_8(1-2\nu)$, $d_{10m} = md_{1m}/a$.

$e_{1m} = m/(1-2\nu)a$, $e_{3m} = -m\alpha(1+\nu)/(1-\nu)a^2$,
$e_{6m} = -2m\{(1-\nu)^2/(1-2\nu)+\alpha/a^2\}/(1-\nu)a^2-2\alpha_{3m}/C(1-\nu)a^2$,
$e_{8m} = 2\nu m/(1-2\nu)a$, $e_{10m} = 2m^2\{(1-\nu)^2/(1-2\nu)+\alpha/a^2\}/(1-\nu)a^2$
$+ 2\alpha_3/C(1-\nu)a^2$, $e_{12m} = 2\alpha_3/C(1-\nu)a-2\alpha m^2/(1-\nu)a^3$.

$f_{3m} = m(1+\nu)/(1-\nu)a$, $f_{6m} = 2m\{1/a^2-\alpha_3/C\alpha\}/(1-\nu)a$,
$f_{10m} = 2\{\alpha_3/C\alpha-m^2/a^2\}/(1-\nu)a$, $f_{12m} = 2m^2/(1-\nu)a^2+2\alpha_3/C\alpha(1-\nu)$.

REFERENCES

[1] P.M. Naghdi, "*Theory of Shells and Plates*", Flugge's Handbuch der Physik, Vol. VI a/2, ed. C. Trusdell, Springer, 1972.

[2] J.H. Havelock, "*The Propagation of Disturbances in Dispersive Media*", Stechert-Hafner Service Agency, New York, 1964.

[3] G.B. Whitham, "*Linear and Nonlinear Waves*", Wiley Interscience, 1975.

[4] J.D. Achenbach, "*Wave Propagation in Elastic Solids*", North Holland Publishing Company, 1973.

[5] M. Kline and I. Kay, "*Electromagnetic Theory and Geometrical Optics*", Wiley Interscience, New York, 1965.

[6] T.Y. Thomas, "*Plastic Flow and Fracture of Solids*", Academic Press, 1961.

[7] C.F. Truesdell, and R.A. Toupin, "*The Classical Field Theories*", Flugge's Handbuch der Physik, Vol. III/1, Springer, 1960.

[8] F.G. Friedlander, "*Sound Pulses*", Cambridge University Press, 1958.

[9] R. Courant and D. Hilbert, "*Methods of Mathematical Physics*", Vol. II, Interscience Publishers, 1966.

[10] F.C. Karal and J.B. Keller, "*Elastic Wave Propagation in Homogeneous and Inhomogeneous Media*", JASA, Vol. 31, No. 6, June 1959, pp. 694-705.

[11] H. Cohen, "*Wave Propagation in Elastic Plates*", Journal of Elasticity, Vol. 6, No. 3, July 1976, pp. 245-259.

[12] J.N. Goodier and W.E. Jahsman, "*Propagation of a Sudden Rotary Disturbance in an Elastic Plate in Plane Stress*", Trans. ASME, Vol. 78, 1956, pp. 284-286.

[13] K. Graff, "*Wave Motion in Elastic Solids*", Clarendon Press, Oxford, 1975.

[14] H. Cohen, "*Wave Propagation in the Linear Theory of Elastic Shells*", Journal of App. Mech., Trans. ASME, June 1976, pp. 281-285.

[15] F. Mainardi and G. Turchetti, "*Wavefront Expansions and Padē Approximants for Transiēnt Waves in Linear Dispersive Media*", Lecture Notes in Physics - Padé Approximants Methods and its Applications to Mechanics - Springer-Verlag, New York, 1976.

[16] V.H. Kenner, W. Goldsmith and J.L. Sackman, "*Longitudinal Impact on a Hollow Cone*", Journal of App. Mech., Trans. ASME, Sept. 1969, pp. 445-450.

[17] B.A. Boley and C.C. Chao, "*Some Solutions of the Timoshenko Beam Equations*", J. App. Mech., Vol. 22, 1955, pp. 579-586.

[18] R.W. Mortimer, J.L. Rose and P.C. Chou, "*Longitudinal Impact of Cylindrical Shells*", Experimental Mechanics, Vol. 12, No. 1, January 1972, pp. 25-31.

[19] J.L. Rose, R.W. Mortimer and A. Blum, "*Elastic-Wave Propagation in a Joined Cylindrical-Conical-Cylindrical Shell*", Experimental Mechanics, Vol. 13, No. 4, April 1973, pp. 150-156.

[20] N.A.N. Youssef and N. Popplewell, "*A Theory of the Greatest Maximum Response of Linear Structures*", Journal of Sound and Vibration, Vol. 56, No. 1, 1978, pp. 21-33.

[21] H. Cohen and A.B. Berkel, "*Wave Propagation in Conical Shells*", Journal of App. Mech., Trans. ASME, December 1972, pp. 1166-1168.

[22] D.P. Billington, "*Thin Shell Concrete Structures*", McGraw-Hill, U.S.A., 1965.

[23] A.O. Awojobi and O.A. Sobaya, "*Ground Vibrations Due to Seismic Detonation of a Buried Source*", Earthquake Eng. and Struct. Dynamics, Vol. 5, 1977, pp. 131-143.

[24] C.L. Pekeris and H. Lifson,"*Motion of the Surface of a Uniform Elastic Half-Space Produced by a Buried Pulse*", JASA, Vol. 29, No. 11, March 1957, pp. 1233-1238.

[25] T.L. Geers and L.H. Sobel, "*Analysis of the Transient Response of Shell Structures by Numerical Methods*", in "*Dynamic Response of Structures*", Proc. of a Symposium held at Stanford Univ. Calif., June 1971, pp. 139-158.

[26] A.S. Veletsos, N.M. Newmark and C.V. Chelapati, "*Deformation Spectra for Elastic and Elastoplastic Systems Subjected to Ground Shock and Earthquake Motions*", Proc. Third World Conf. on Earthquake Eng. Vol. II, New Zealand, 1965, pp. 663-680.

[27] G.R. Walker, "*Earthquake Resistant Design - The Pulse Method*", Proc. Third World Conf. on Earthquake Eng. Vol. II, New Zealand, 1965, pp. 683-694.

[28] J.W.S. Rayleigh, "*The Theory of Sound*", Vols. I and II, Dover Publications, New York, 1945.

[29] A.E.H. Love, "*Theory of Elasticity*", Cambridge Univ. Press, London, 4th Ed., 1927.

[30] R.D. Mindlin and G. Herrmann, "*A One-Dimensional Theory of Compressional Waves in an Elastic Rod*", Proc. 1st U.S. Natn. Congr. App. Mech., 1950, pp. 187-191.

[31] S.P. Timoshenko, "*On the Correction for Shear of the Differential Equation for Transverse Vibration of Prismatic Bars*", Phil. Mag., Ser. 6, 41, 744, 1921.

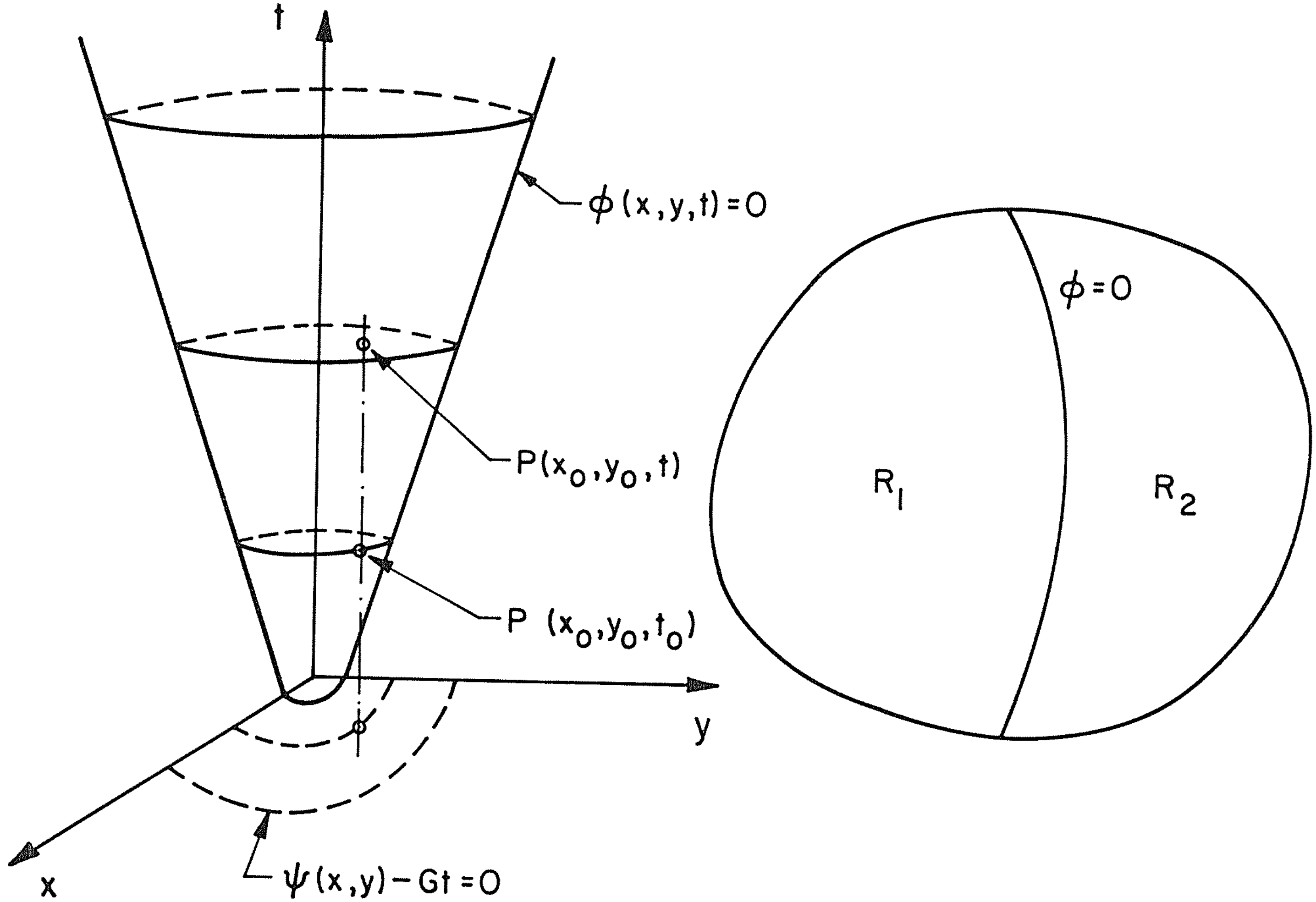

(a)

(b)

Fig. 1. The Surface of Discontinuity.

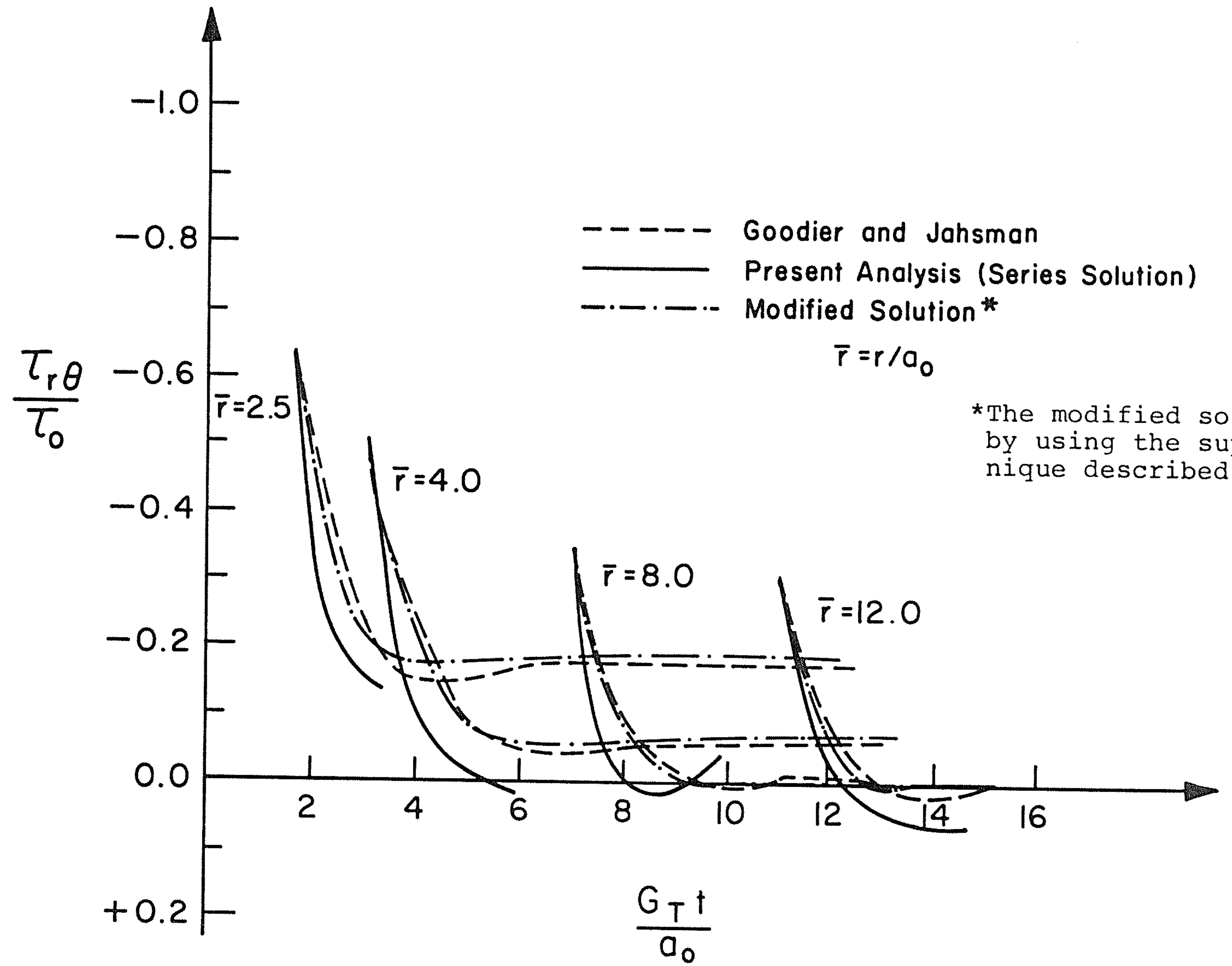

*The modified solution was obtained by using the superposition technique described in Ch. III.

Fig. 2 . Variation of Shear Stress in the Plate

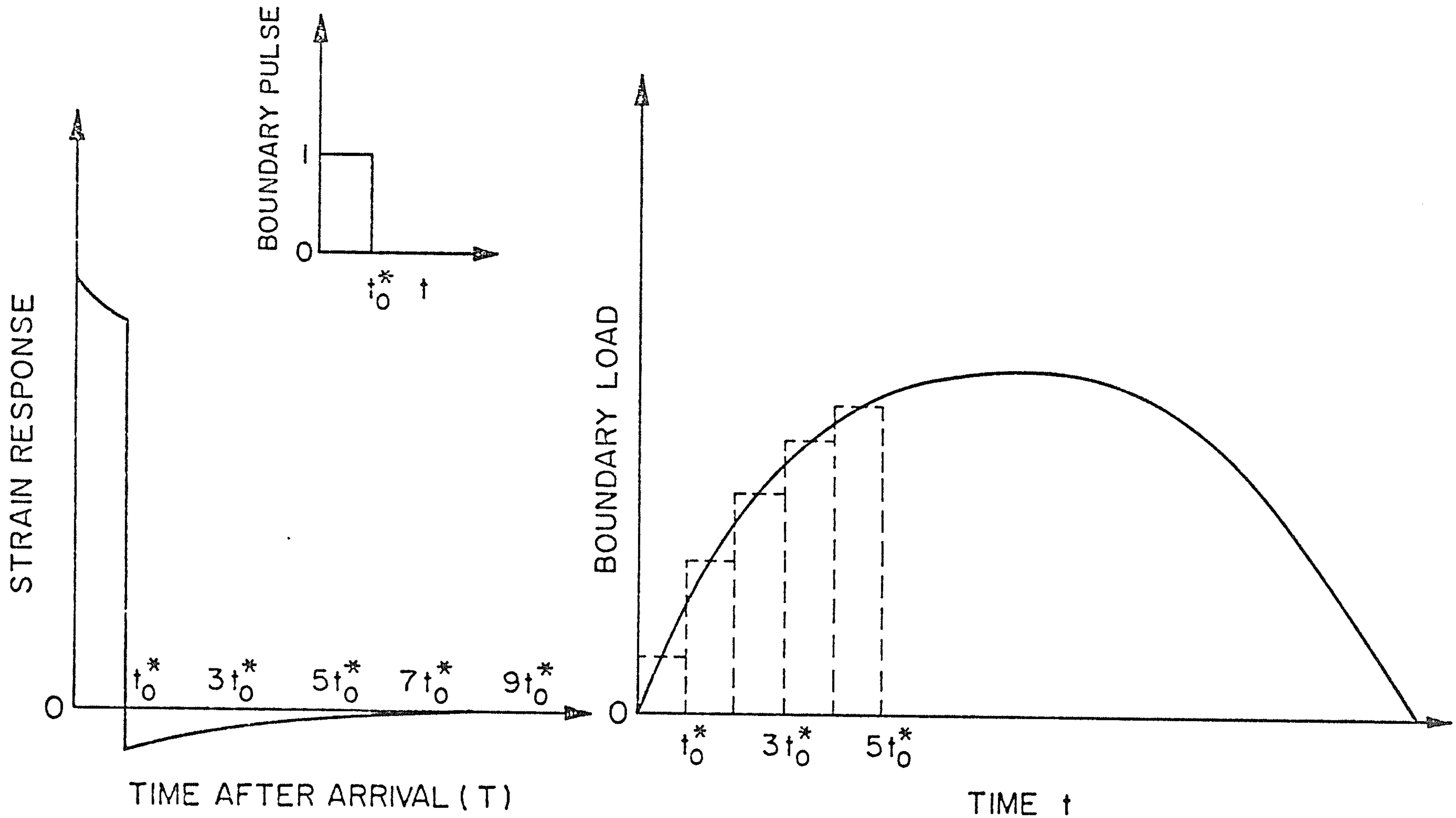

(a) Typical Test Solution .

(b) Equivalent Step Pulses of Duration t_o^*

Fig. 3 . Numerical Superposition Technique

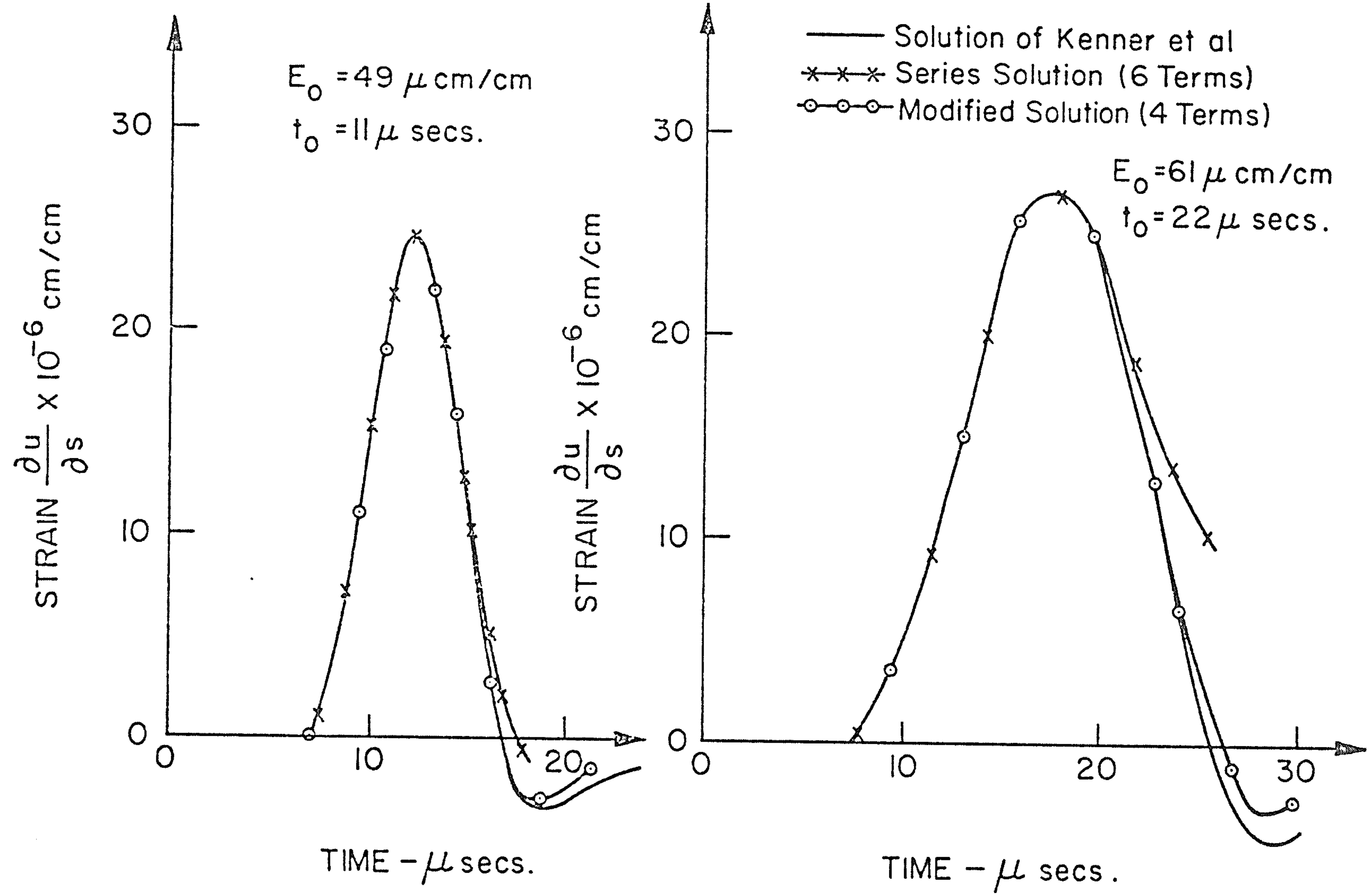

Fig. 4a. Strain Response in the Conical Shell. (s = 5.6 cms)

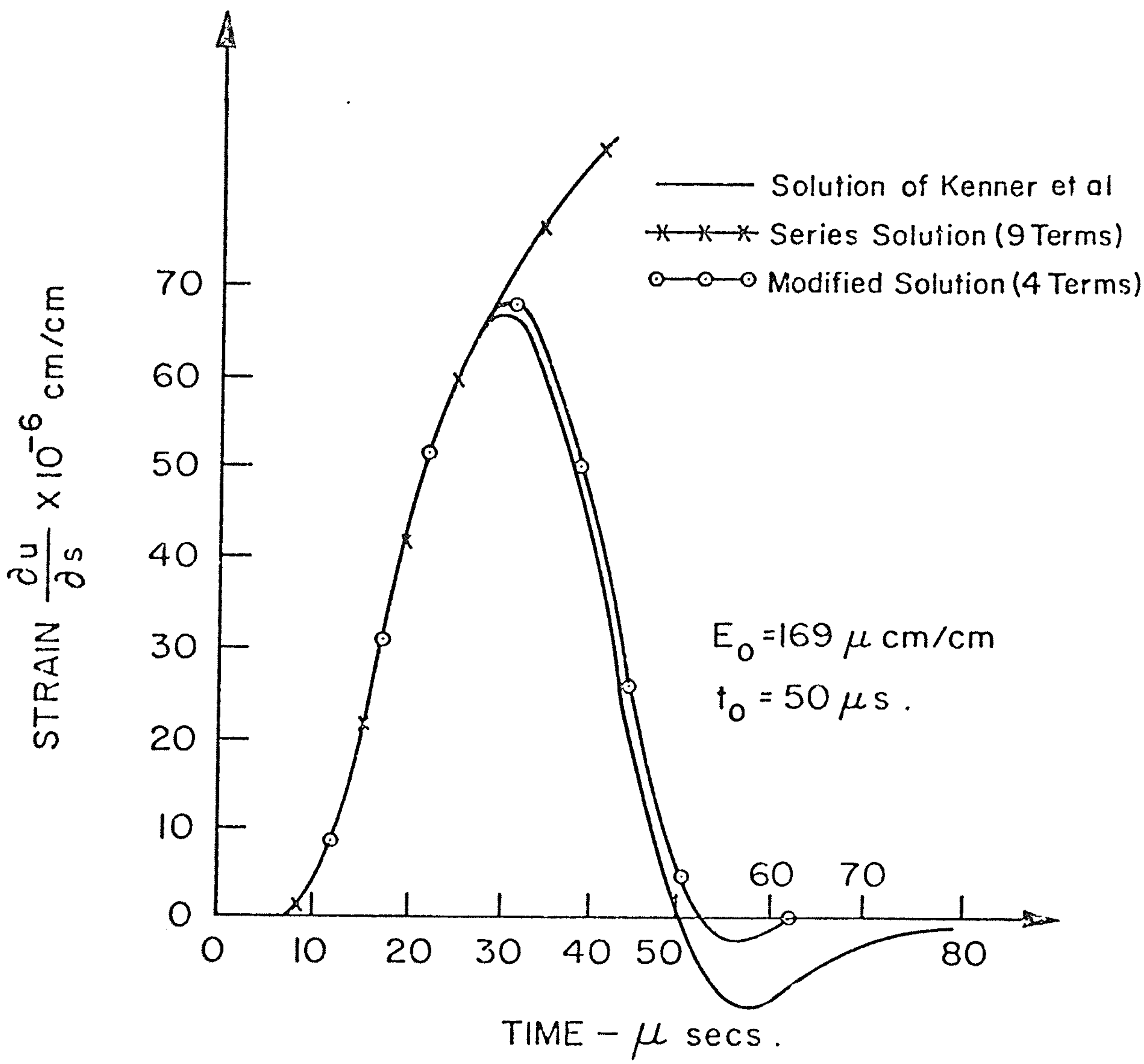

Fig. 4b. Strain Response in the Conical Shell
(s = 5.6 cms)

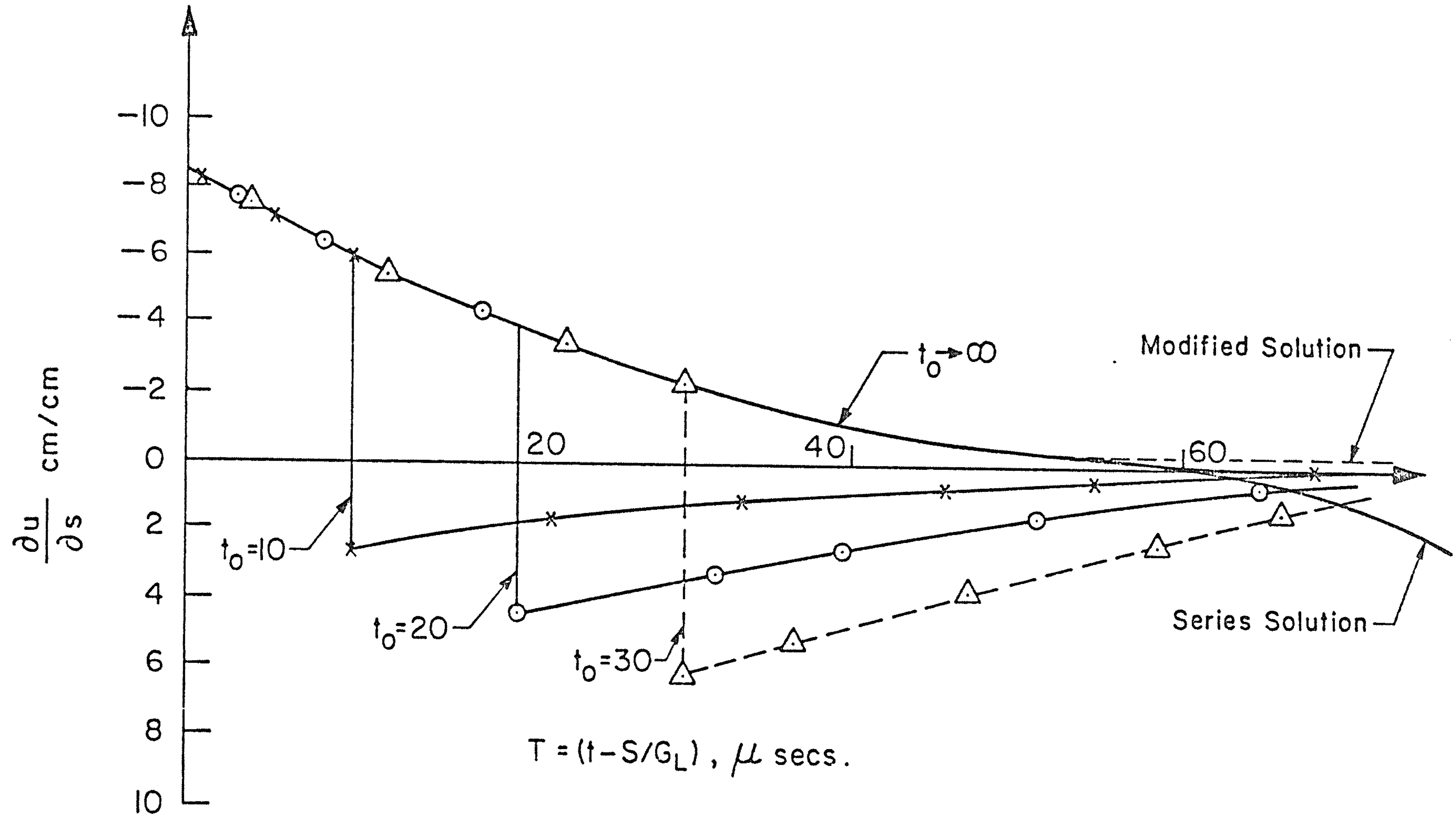

Fig. 5. Strain Response in the Cylindrical Shell due to Velocity Pulses.
(s=3.05m)

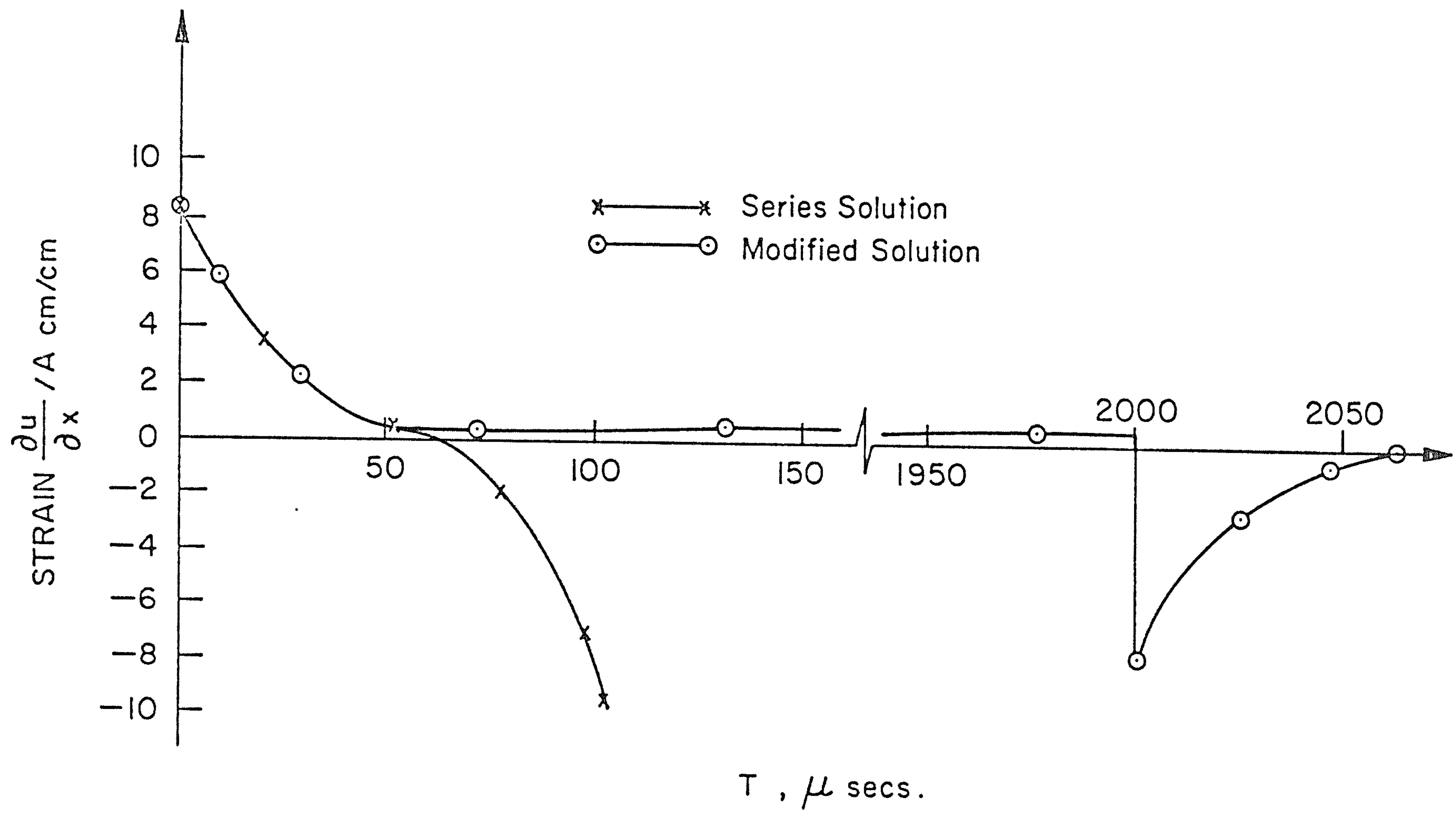

Fig. 6 . Strain Response in the Cylindrical Shell due to a Blast Pulse (s=3.05 m)

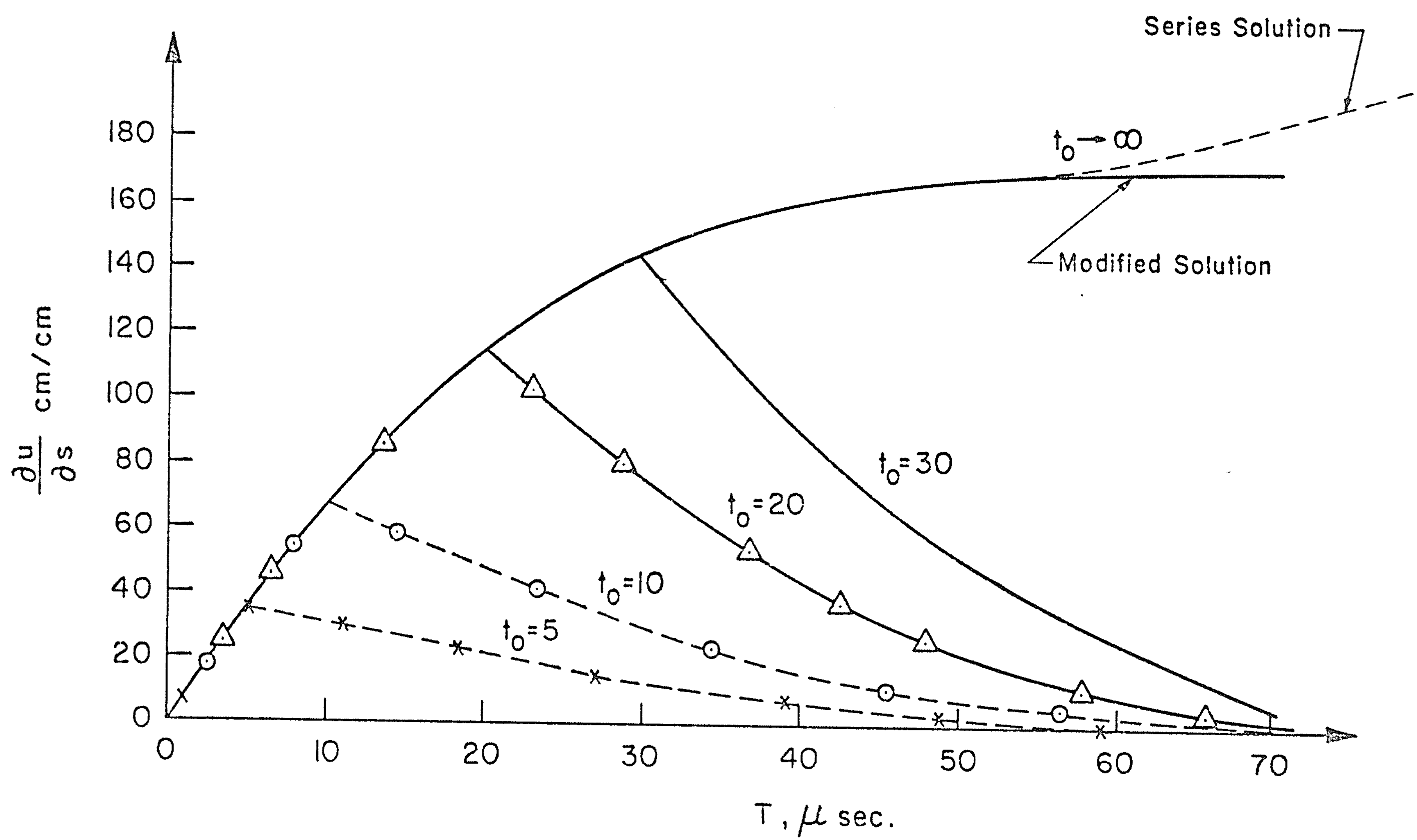

Fig. 7. Strain Response in the Cylindrical Shell due to Acceleration Pulses.
(s = 3.05m)

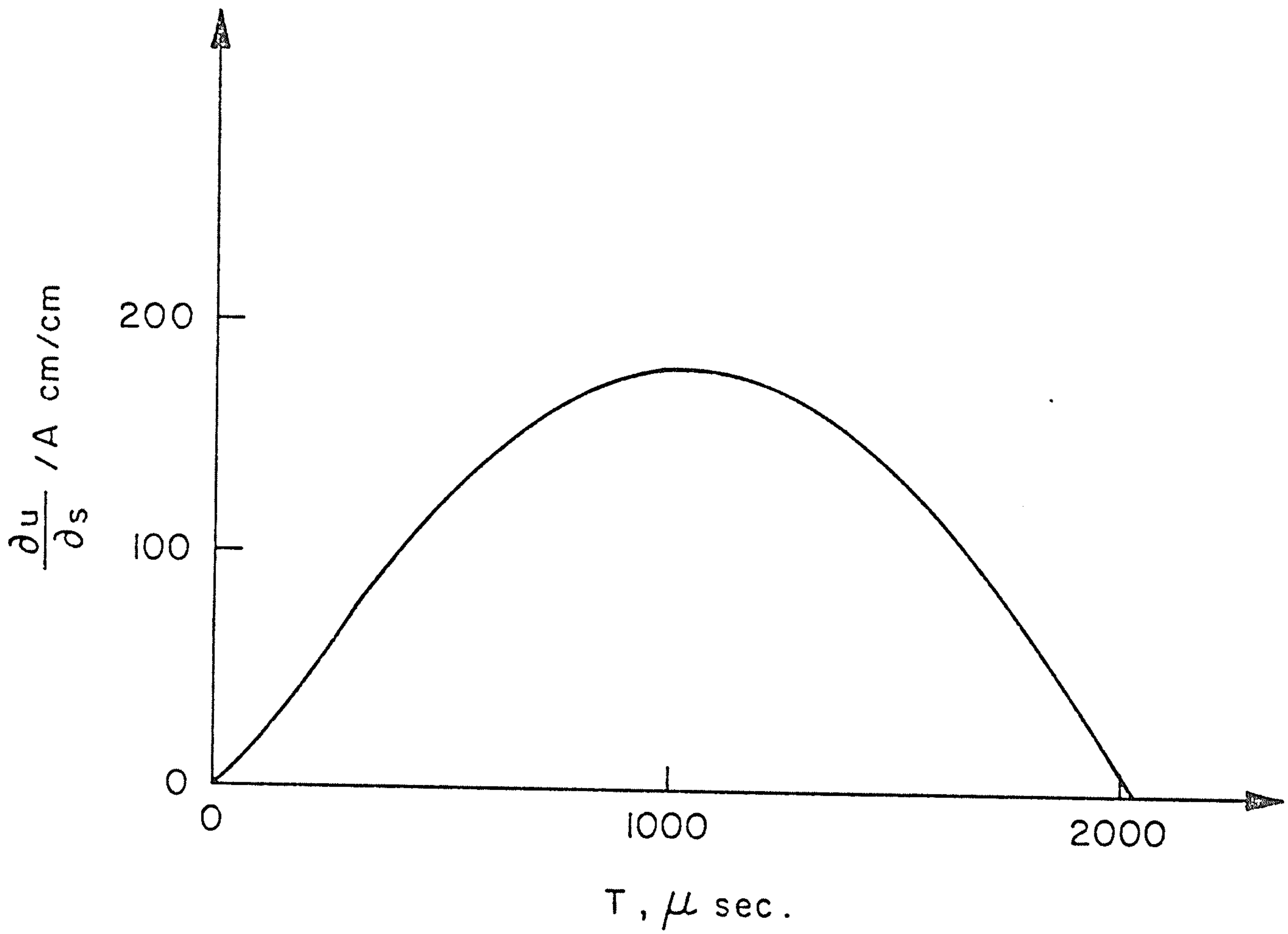

Fig. 8 . Strain Response in a Cylindrical Shell due to Vertical Ground Excitation . (s=3.05 m) .

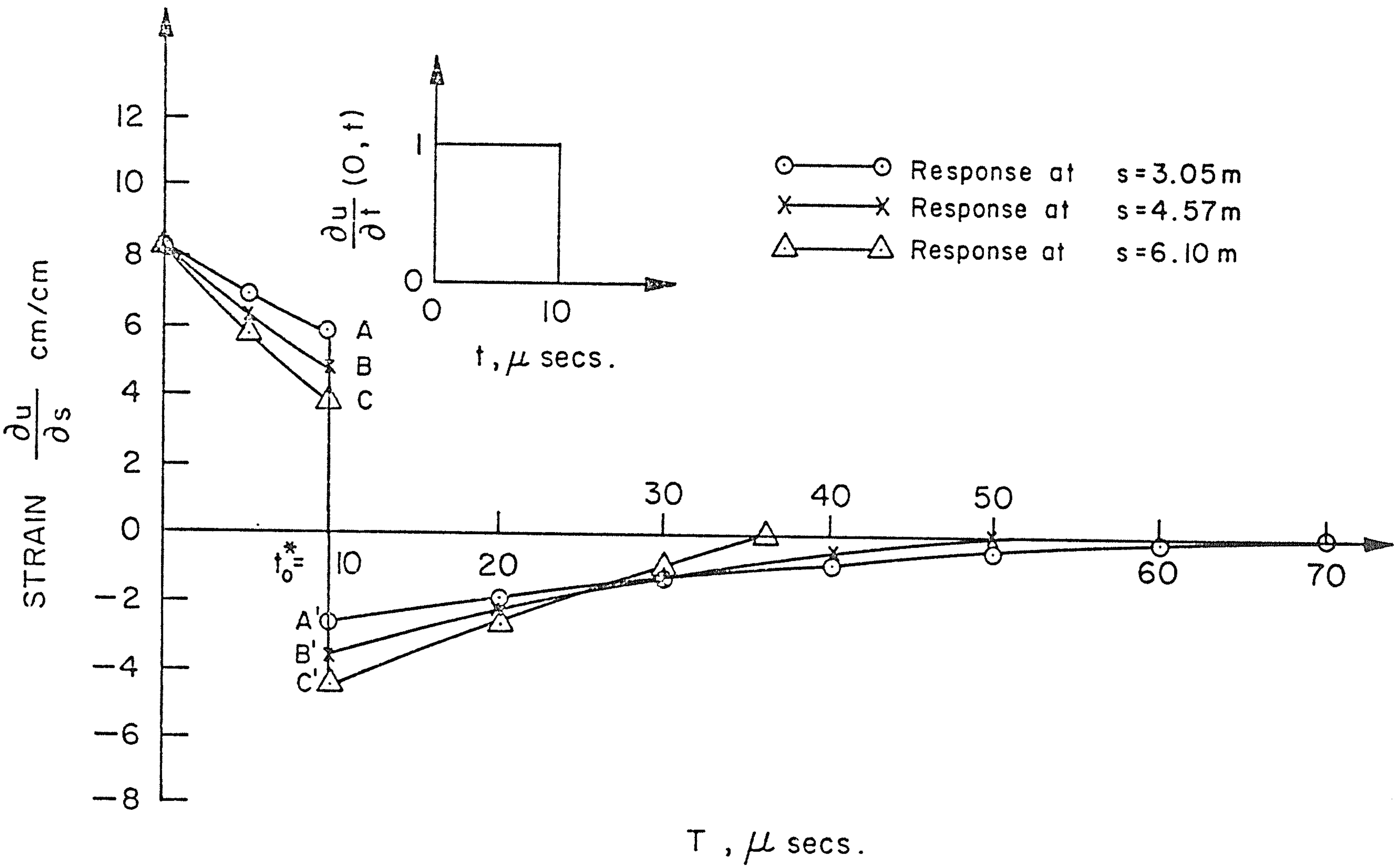

Fig. 9. Test Solutions for a Cylindrical Shell (Example 2)

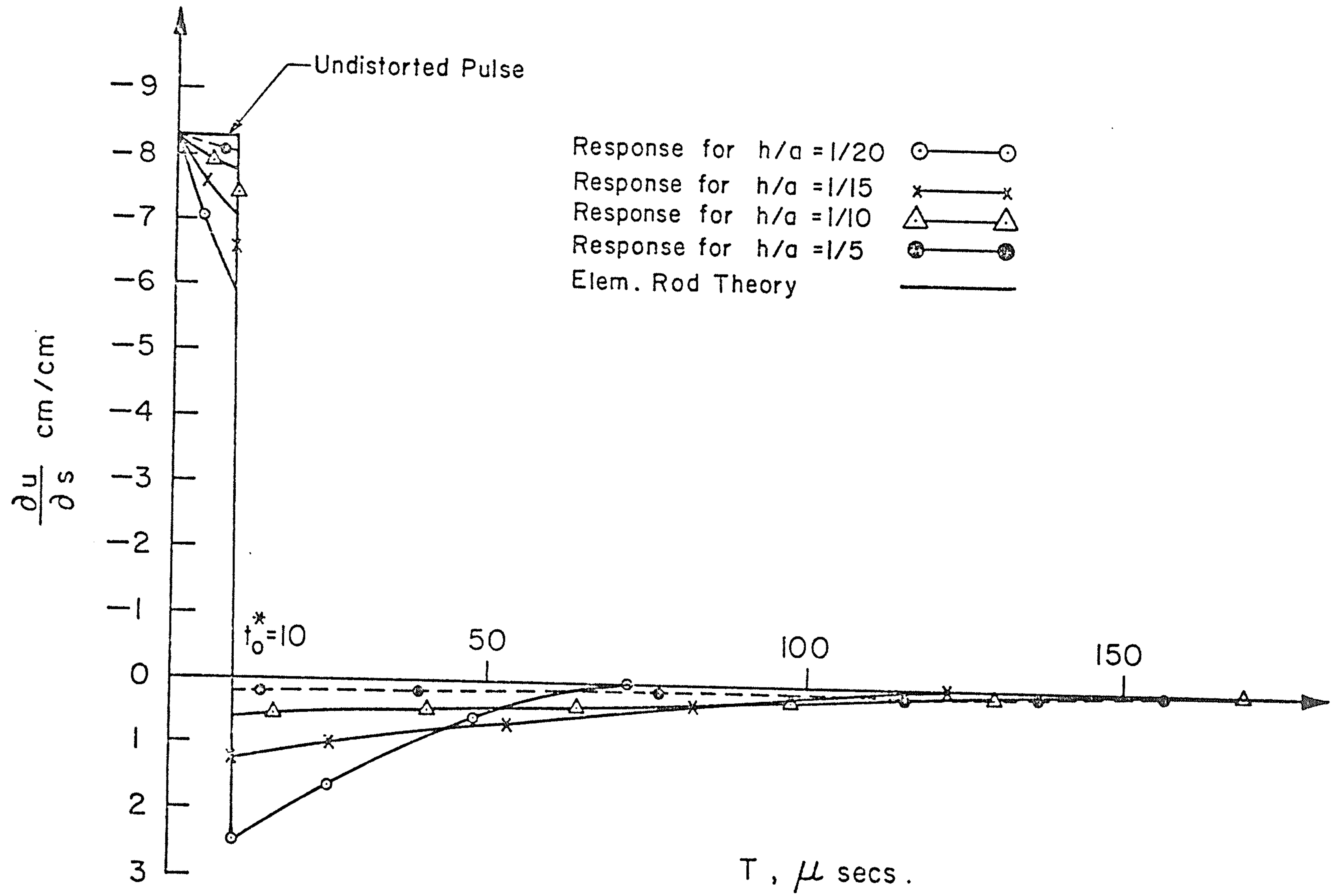

Fig. 10. Test Solutions for Different h/a Ratios. (s=3.05m)

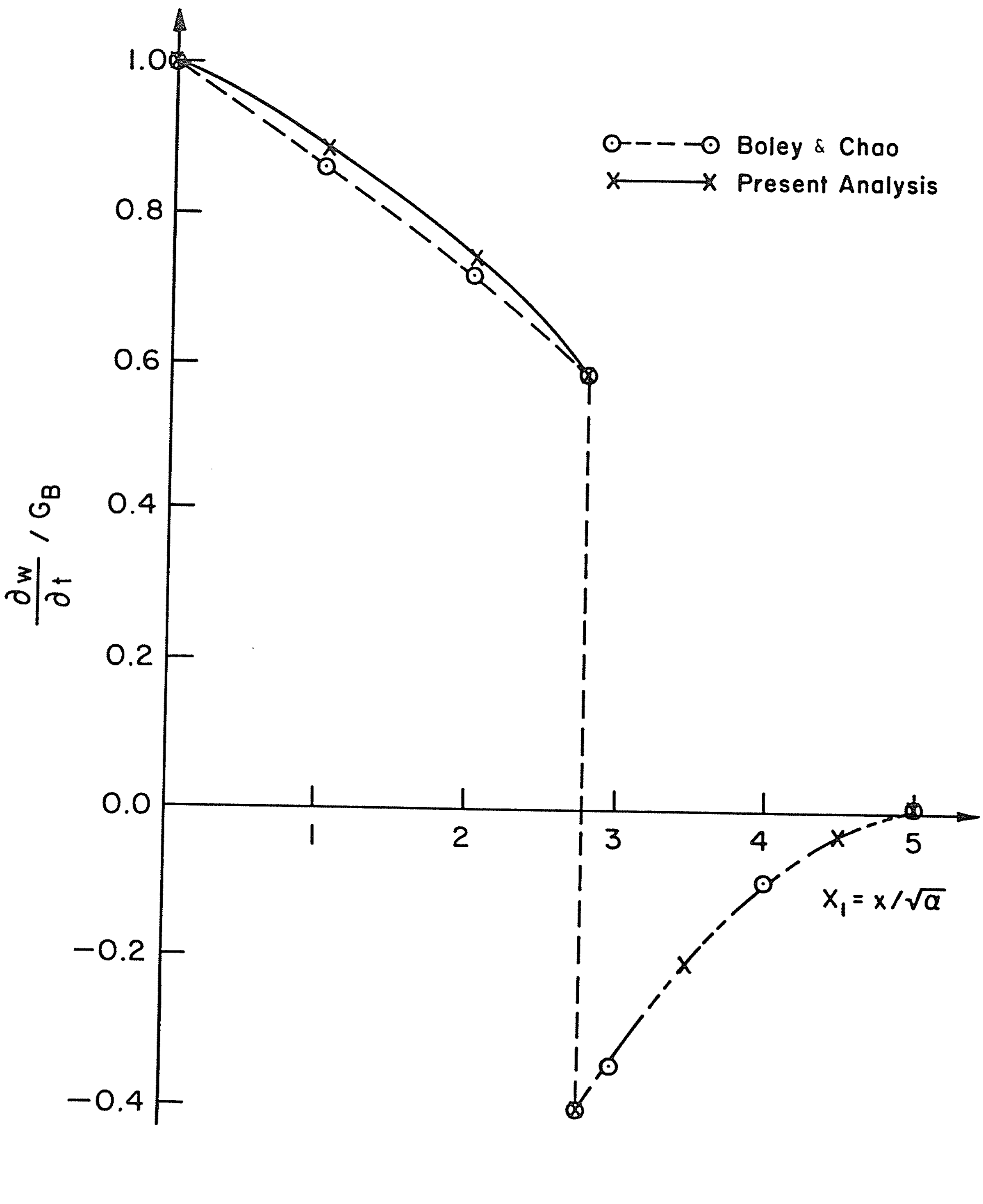

Fig. 11. Variation with Position of the Velocity ($t_1 = G_B t/\sqrt{\alpha} = 5$)

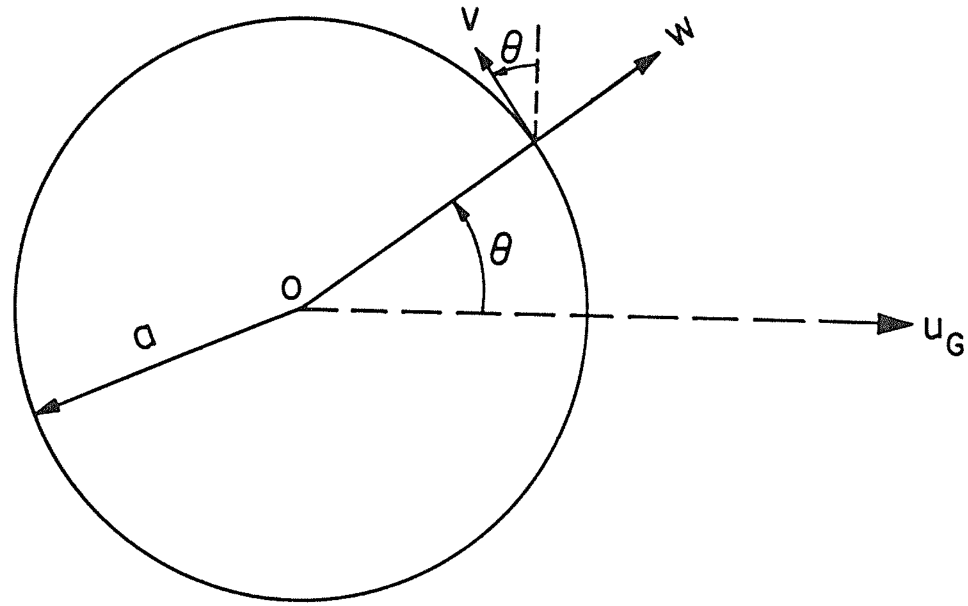

Fig. 12. Boundary Conditions for Horizontal Ground Excitation

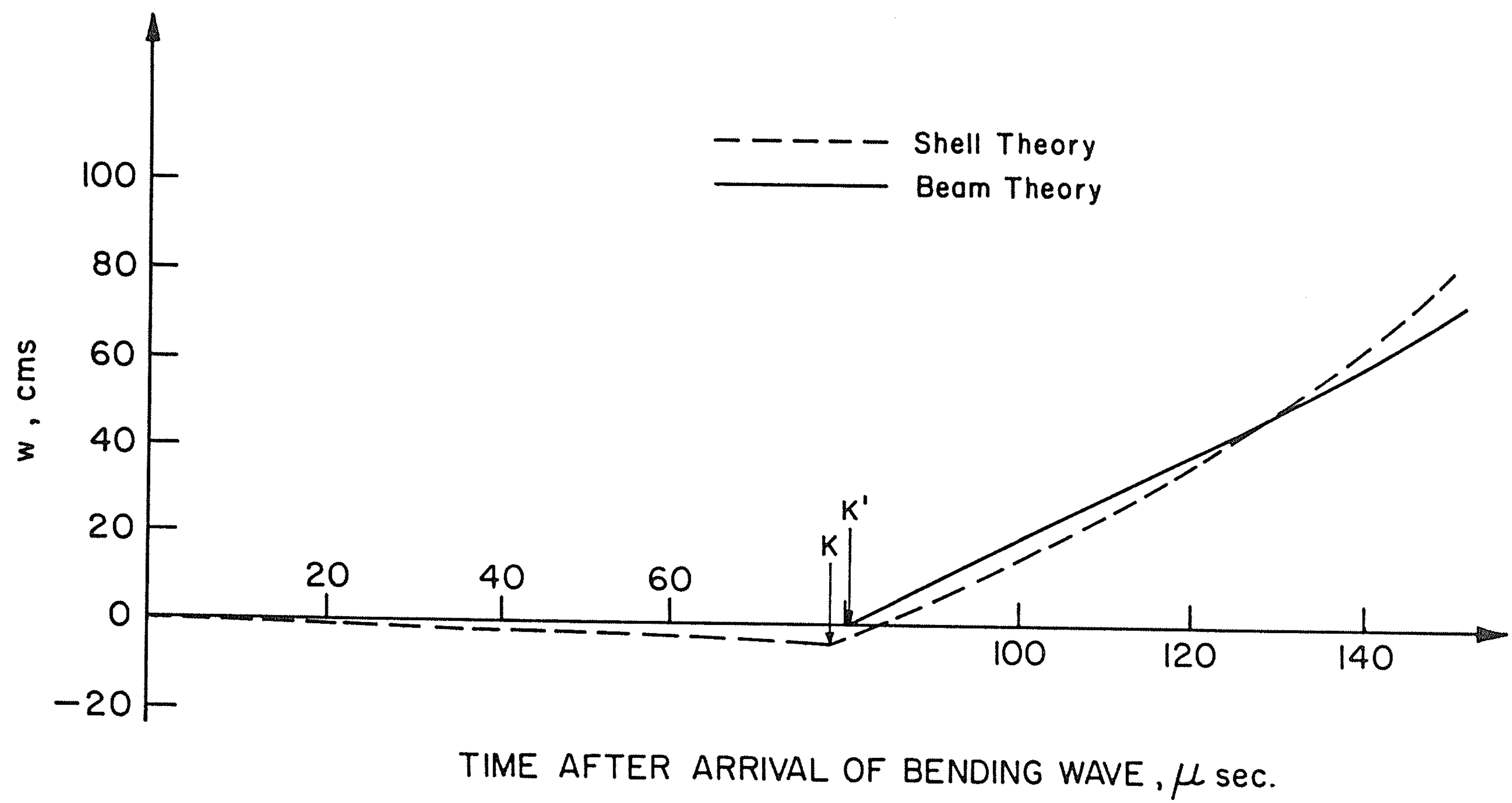

Fig. 13. Radial Displacement w ($s = 30.5$ cms , $\theta = 0°$)

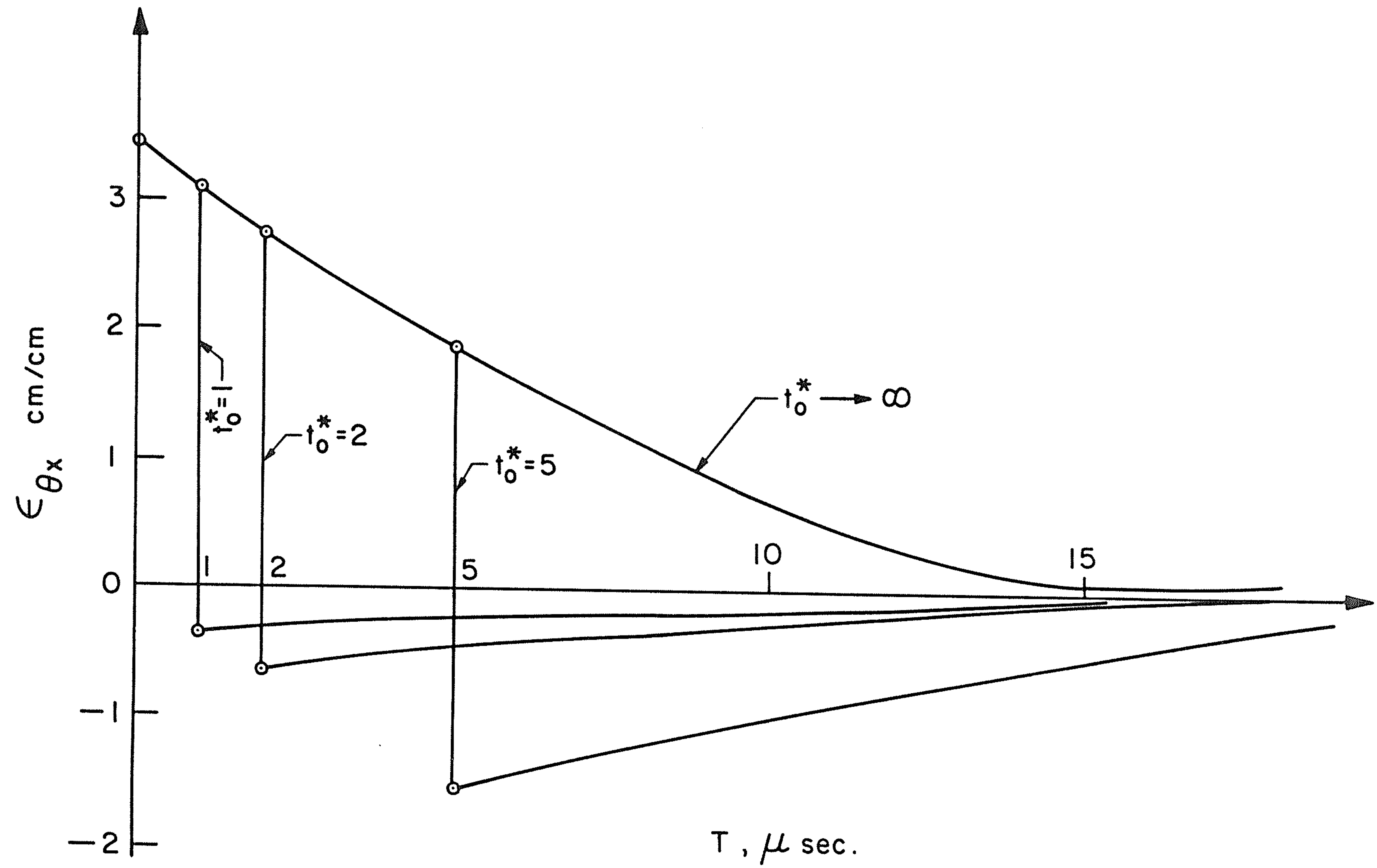

Fig. 14. Test Solutions for Strain $\epsilon_{\theta x}$ – Velocity Boundary Condition ($x=3.05m, \theta=90°$)

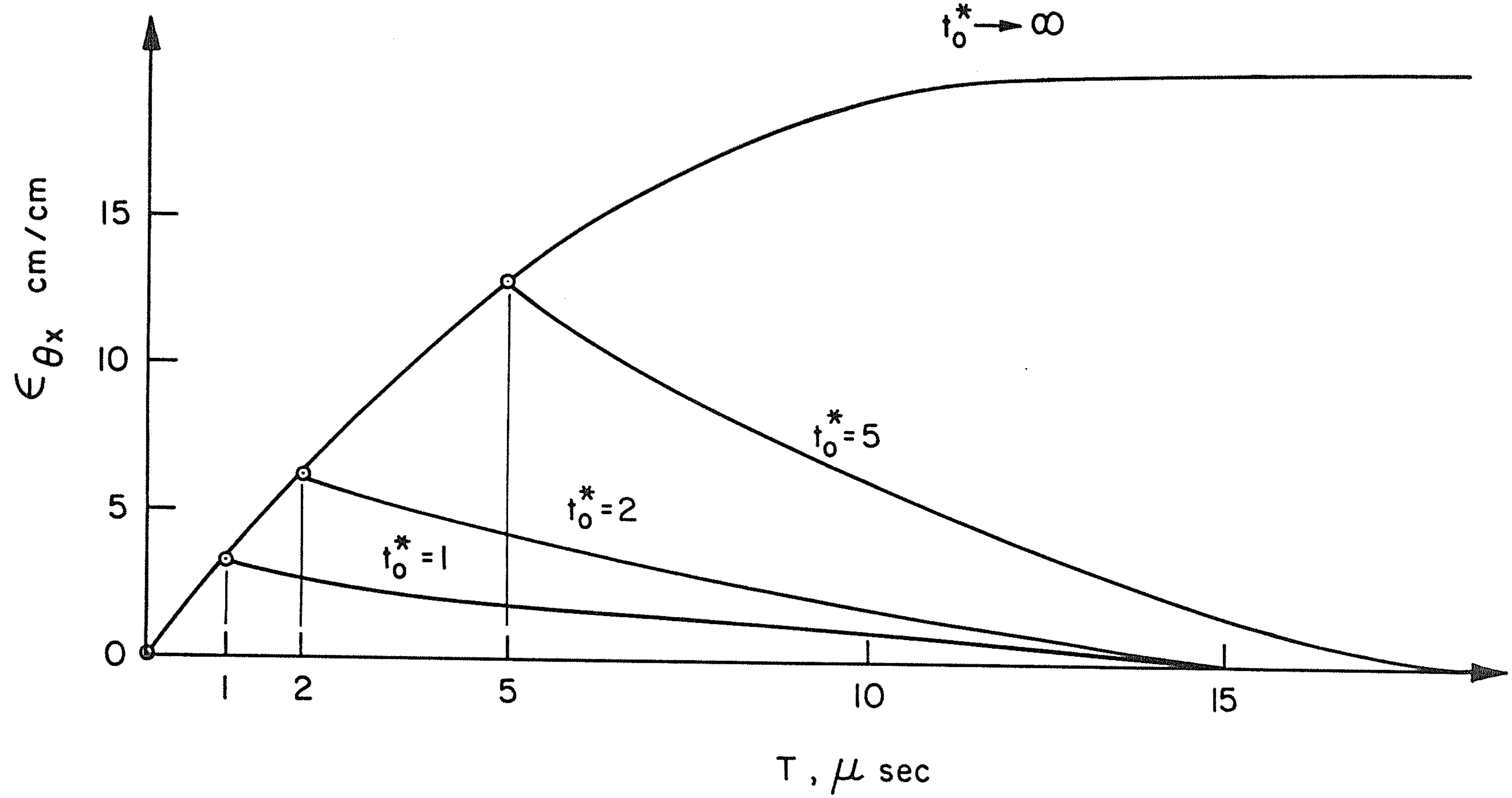

Fig. 15. Test Solutions for Strain ϵ_{θ_x} — Acceleration Boundary Condition ($x = 3.05$ m, $\theta = 90°$)